

ANALYSIS OF SIBC/IBSC AND MAZE/MAZF, TWO CHROMOSOMALLY-
ENCODED TOXIN-ANTITOXIN SYSTEMS IN *ESCHERICHIA COLI*

by

MARLY IVETTE ROCHE RIOS

(Under the Direction of Sidney R. Kushner)

ABSTRACT

Toxin-antitoxin (TA) modules are found in both bacterial plasmids and genomes.. They ensure plasmid maintenance via a mechanism known as post-segregational killing. However the biological importance of the large number of chromosomal TA loci identified thus far is still the subject of great debate. Some have been linked to stress response, biofilm formation, persistence, and development, but many systems still need to be characterized.

Here we have examined the biogenesis and decay of the Type I toxin-antitoxin system SibC/*ibsC*. SibC is a *cis*-encoded sRNA that prevents the toxic effect of the IbsC protein by binding to its mRNA and inhibiting its translation. We have shown that ribonucleases RNase E, RNase III, and RNase P all play a role in SibC biogenesis and decay. Interestingly, we have also demonstrated a role for Hfq in the stability of SibC and its regulatory effect on *ibsC*. These findings suggest that gene expression regulation mediated by *cis*-encoded sRNAs is more complicated and shares more features with *trans*-encoded sRNA regulation than previously thought.

We have also analyzed the role of MazF, an mRNA interferase encoded by the Type II toxin-antitoxin system *mazEF*, in general mRNA decay. Surprisingly, we have shown that although MazF does not play a role in general mRNA in *E.coli*, a deletion of the downstream gene MazG does. MazG has been shown to regulate the stringent response by lowering the levels of ppGpp, the alarmone that redirects transcription to allow the cells to survive nutrient starvation. The link between the stringent response, MazG, and mRNA needs to further analyzed.

INDEX WORDS: Toxin-antitoxin systems, sRNAs, RNA interferases, *Escherichia coli*

ANALYSIS OF SIBC/IBSC AND MAZE/MAZF, TWO CHROMOSOMALLY-
ENCODED TOXIN-ANTITOXIN SYSTEMS IN *ESCHERICHIA COLI*

by

MARLY IVETTE ROCHE RIOS

BS, Interamerican University of Puerto Rico, 2003

A Dissertation Submitted to the Graduate Faculty of The University of Georgia in Partial
Fulfillment of the Requirements for the Degree

DOCTOR OF PHILOSOPHY

ATHENS, GEORGIA

2013

© 2013

Marly Ivette Roche Ríos

All Rights Reserved

ANALYSIS OF SIBC/IBSC AND MAZE/MAZF, TWO CHROMOSOMALLY-
ENCODED TOXIN-ANTITOXIN SYSTEMS IN *ESCHERICHIA COLI*

by

MARLY IVETTE ROCHE RIOS

Major Professor: Sidney R. Kushner

Committee: Marcus Fechheimer
Anna C. Glasgow Karls
Michael McEachern
Richard B. Meagher

Electronic Version Approved:

Maureen Grasso
Dean of the Graduate School
The University of Georgia
May 2013

DEDICATION

To my sister, Isis. I wouldn't have made it here without you. To my husband,
Jimmy. I wouldn't have made out without you.

ACKNOWLEDGEMENTS

I would first like to thank my dissertation advisor Dr. Sidney Kushner for welcoming me into his lab with arms wide open and for helping me become the scientist I am today.

I would also like to acknowledge Dr. Mary Bedell for teaching me about doing science with passion, Dr. Marcus Fechheimer who was with me from the very beginning keeping motivated through it all, and the rest of my advisory committee, Dr. Anna Karls, Dr. Mike McEachern, and Dr. Rich Meager for their advice and guidance throughout this process.

I want to thank the past and present members of the Kushner lab for making the workload bearable and the work environment enjoyable. A special thank you to Sarah for introducing me to the world of sRNAs, to Ankito for saving me countless hours by starting my overnights and for listening to me as I try to make sense of my data, and to Katie for taking care of me throughout the years and the endless hours of pampering (even if we looked like monkeys grooming!).

I want to thank all of my “families”, for without them none of this would have been possible. There are no words to describe the love and gratefulness I feel towards my parents, Ivette y Manuel, and my sisi, Isis. You are the wind beneath my wings. All I have accomplished and will accomplish in life is because of you. I am grateful to my grad school friends, some of which I now consider family, because whether you came into my life for a reason, a season, or a lifetime, you have made it better. And last, but not least, I

want to thank my loving husband, Jimmy (BD), for always reminding me that “no matter what, it will be okay”, for having a sweet mother that loves me and takes care of me as if I was her own, and for giving me the greatest gift of all, my own family.

¡Todo lo pude en Dios que me fortaleció!

TABLE OF CONTENTS

	Page
ACKNOWLEDGEMENTS	v
LIST OF TABLES	viii
LIST OF FIGURES.....	ix
CHAPTER	
1 INTRODUCTION AND LITERATURE REVIEW.....	1
2 ANALYSIS OF THE SIBC/ <i>IBSC</i> TOXIN-ANTITOXIN SYSTEM IN <i>ESCHERICHIA COLI</i>	32
3 THE MRNA INTERFERASE MAZF DOES NOT PLAY A ROLE IN MRNA DECAY IN <i>ESCHERICHIA COLI</i>	79
4 CONCLUSIONS.....	107

LIST OF TABLES

	Page
Table 2.1: Bacterial strains and plasmids used in this study	64
Table 2.2: Oligos used in this study	67
Table 2.3: SibC half-lives in the presence and absence of <i>ibsC</i> expression.....	68
Table 2.4: SibC half-lives in <i>hfq</i> mutants	69
Table 3.1: Bacterial strains used in this study.....	99
Table 3.2: Oligos used in this study	100
Table 3.3: mRNA half-lives of various strains containing the $\Delta mazEFG$ deletion in the W3110 genetic background.....	101
Table 3.4: mRNA of half-lives in $\Delta mazF$ strains.....	102

LIST OF FIGURES

	Page
Figure 2.1: Description of the <i>SibC</i> and <i>IbsC</i> plasmids used in this study.....	70
Figure 2.2: Steady-state analysis of <i>SibC</i> in early-stationary phase cultures at 30°C and 44°C.....	71
Figure 2.3: Steady-state analysis of <i>SibC</i> and <i>ibsC</i> at 44°C.....	72
Figure 2.4: Half-lives of <i>SibC</i> 141 in the presence and absence of its target, <i>ibsC</i>	73
Figure 2.5: Half-lives of <i>SibC</i> 141 in RNase E and Hfq mutants.....	74
Figure 2.6: Half-lives of <i>ibsC</i>	75
Figure 2.7: <i>SibC</i> processing after <i>ibsC</i> induction	76
Figure 2.8: <i>IbsC</i> processing in the absence of <i>SibC</i>	77
Figure S.2.1: Overexposed Northern blot of <i>SibC</i> shown in Figure 2.2	78
Figure 3.1: mRNA half-life of <i>rpsO</i> in $\Delta mazEFG$ deletion strains in the MG1693 genetic background	103
Figure 3.2: Comparison of growth properties of <i>rne-1</i> and <i>rne-1</i> $\Delta mazEFG$ mutant strains in the MG1693 and W3110 genetic backgrounds	104
Figure 3.3: mRNA half-lives of <i>rpsO</i> and <i>cspE</i> in $\Delta mazEFG$ deletion strains in the W3110 genetic background.....	105
Figure 3.4: mRNA half-lives of <i>rpsO</i> and <i>cspE</i> in $\Delta mazF$ strains in the W3110 genetic background.....	106

CHAPTER 1

INTRODUCTION AND LITERATURE REVIEW

INTRODUCTION

Toxin-antitoxin (TA) modules were first identified in plasmids in the 1980s. They consist of a stable toxin protein capable of killing cells and/or causing cell stasis and an antitoxin that specifically inhibits its toxic effect. Due to the unstable nature of the antitoxins, TA modules provide a mechanism to ensure plasmid maintenance in growing cultures. Cells that fail to inherit a plasmid containing the TA locus quickly lose the antitoxin, which allows the toxic proteins to kill the plasmid-free cells (1,2). This process is known as post-segregation killing (PSK).

Since their discovery, numerous TA systems have been discovered in bacterial and archaeal genomes. To date, at least 34 TA systems have been identified in *E.coli* (3). Although their chromosomal roles are still the subject of great debate, evidence indicates that they are involved in several cellular functions including stress response, biofilm formation, persistence, and even development (4-6).

Prokaryotic toxin-antitoxin systems are classified according to the nature and mechanism of action of the antitoxin. Thus far, five types (Types I – V) of TA systems have been identified. Type I TA systems are characterized by preventing toxicity via small regulatory RNAs (sRNAs). The antitoxin sRNA base pairs with the mRNA encoding the toxin and prevents its translation. In Type II systems, the antitoxin is a

protein that binds to the toxic peptide and neutralizes its activity. These two types of toxin regulation are by far the most abundant.

Only one example of a Type III toxin-antitoxin system has been characterized thus far. In the ToxI-ToxN TA system, inhibition is achieved by the binding of the ToxI RNA to the ToxN toxic protein, forming an RNA-protein complex (7). The ToxI antitoxin is a 5.5 tandem repeat of a 36 nucleotide sequence that forms pseudoknots, while ToxN is a endoribonuclease related to Kid and MazF (8). In *Erwinia*, this system seems to be involved in abortive infection, a mechanism to prevent phage replication by promoting cell death (9). Using a combination of structure and sequence homology, approximately 125 Type III TA loci have been predicted across three Phyla, suggesting that this type of system is widespread (10).

Two additional toxin-antitoxin systems have been recently identified in *E.coli* and two new families have been proposed. CptA-CptB is the only known type IV TA. CptA (cytoskeleton polymerization inhibiting toxin), formerly known as YeeV, is the first membrane-associating toxin found in a bacterial toxin-antitoxin system and the first one to inhibit cell growth by interfering with cytoskeletal proteins (11,12). CptA interacts and prevents the polymerization of FtsZ and MreB, two essential cytoskeletal proteins, and is inhibited by CptB (13). However, the mechanism of toxin neutralization by type IV antitoxins has yet to be determined, since no physical interactions between the toxins and the antitoxins have been detected (13).

GhoS, the only type V antitoxin known to date, has been shown to inhibit GhoT production (toxin-producing *ghost* cells) by cleaving its mRNA (14). When

overexpressed, GhoT disrupts the cell membrane and causes the center of dying cells to appear transparent while the poles look dense. This is the first documented case of an antitoxin with ribonuclease activity (14).

This review focuses on key aspects of the discovery, classification, and function of type I and type II prokaryotic toxin-antitoxin systems, since these systems are the best studied.

Type I toxin-antitoxin systems

In Type I toxin-antitoxin (TA) systems, translation of the toxic peptide is inhibited by the base-pairing of an antitoxic RNA molecule to the mRNA encoding the toxin. In Type I TA systems, most sRNAs inhibit the expression of small (less than 60 amino acids), hydrophobic toxins that target the cell membrane and inhibit ATP synthesis (15). The inhibitory antisense RNAs are usually *cis*-encoded, encoded on the opposite strand of the target, and they overlap the toxic transcript at either the 5' or the 3' end. However, *trans*-encoded systems where the antitoxin sRNAs are expressed from a loci separate from the toxin and have limited sequence complementarity with their targets, have also been characterized (16). Chromosomally encoded sRNAs have also been shown to play key roles in the regulation of gene expression of non-toxic genes and will be briefly discussed in this review as well (17).

***Cis*-encoded sRNA antitoxins in Gram-negative bacteria**

Hok/Sok was the first toxin-antitoxin system to be characterized and it was discovered due to its role in stable inheritance of plasmids and post-segregational killing (PSK)(1). Hok, a small toxin capable of *host killing*, and Sok, a suppressor of *host killing*

are encoded in the *parB* (*partitioning*) locus on the R1 plasmid (2). This locus has a third gene, *mok* (*modulation of killing*), which overlaps with *hok*. *Sok* is a sRNA encoded in the opposite strand of *hok* and it has complementarity to the translational initiation region (TIR) located at the 5' region of the *mok* mRNA (18). When present, *sok* RNA forms a duplex with the *mok-hok* mRNA, which is quickly degraded by RNase III (19). When the cells lose the plasmid, *sok* is quickly degraded, which allows the *mok-hok* mRNA to be translated. Expression of the Hok toxin damages the cell membrane and induces ghost-cell formation, resulting in PSK of the plasmid-free cells (2).

Flm (*F* leading maintenance) and *SrnB-SrnC* (*stable RNA negative*) are *hok/sok* homologues found in the F plasmid. Similarly, PndA-PndB (*promotion of nucleic acid degradation*), also a *hok/sok* homologue, has been described in plasmid R483 (20,21). In addition, six chromosomal *hok* homologues have been characterized in *E. coli* (22). Interestingly, these loci do not mediate post-segregational killing when cloned into plasmids, like their plasmid-encoded counterparts do (22). The role of these chromosomally-encoded TA systems is still a mystery.

Several chromosomal type I toxin-antitoxin families in *E. coli* were identified by chance and none of them seem to have homology to plasmid sequences. One of these families is composed of four long repetitive elements that were detected by genome sequencing (23). The characterization of one of these LDRs (long direct repeats), LDR-D, revealed that overexpression of LDR-D was lethal to the cells and that its expression was post-transcriptionally regulated by Rdl-D RNA (*regulator detected in LDR-D*). Rrl-D is a sRNA with complementarity to the 5'UTR of *ldrD*. Although the mechanism of

regulation has not been clearly defined, evidence suggests that it is regulated in a manner similar to the Hok/Sok system (23).

The QUAD family of repeats was identified in a genomic search for new intergenic repeats (24). These repeats were called SIBs (*short, intergenic, abundant sequences*) and the toxic genes they repress were renamed *ibs* (*induction brings stasis*). SIBs are constitutively expressed and they are the only antitoxic sRNAs known to date to have complete complementarity to their target mRNAs, the *ibs* coding sequences, including the ribosome binding site (25). *Ibs* overexpression leads to the destabilization of the cell membrane, while Sib RNAs negatively regulate *ibs* transcripts levels (25). How these TA systems are regulated and their biological role in the cell is still an enigma. The only insights into the mechanism of *ibs* regulation by Sib RNAs comes from the observation that in the absence of RNase III, *ibs* mRNA seems to become stabilized. This increase in stability suggests that Sib/*Ibs* duplexes are degraded by RNase III (25). Additionally, the RNA chaperone Hfq does not seem to have an effect on the expression levels of either SibC or *ibsC* (25).

A *cis*-encoded Type I TA system has been shown to be induced by the SOS response to DNA damage, SymR-SymE. The toxin, SymE (SOS-induced *yjiW* gene with similarity to *MazE*), is different from all the other Type I TA toxins known to date. Instead of targeting the cell membrane, SymE is an endoribonuclease that shares structural similarities with MazE, the antitoxic peptide of the Type II MazEF toxin-antitoxin family (26). When overexpressed, SymE reduces cell viability and inhibits protein synthesis in a manner similar to ribosome-independent RNA interferases (see below). It

has been suggested that SymE cleavage of mRNAs helps recycle damaged RNAs and rescue ribosomes (15). In addition, like many Type II antitoxins, SymE is degraded by the Lon protease (26). The *cis*-encoded antitoxin, SymR (*symbiotic RNA*), is transcribed from the opposite strand and it overlaps with the initiation codon and the Shine-Dalgarno sequence of *symE*. SymR is constitutively expressed and it regulates SymE expression post-transcriptionally. The exact mechanism has not been elucidated, but the inhibition is independent of RNase III and the RNA chaperone Hfq (26). Furthermore, *symE* expression is regulated at the transcriptional level by LexA, an SOS-response gene repressor (27).

***Trans*-encoded sRNA antitoxins in Gram-negative bacteria**

Additional Type I toxin-antitoxin systems were discovered in the search for novel sRNAs, by bioinformatics approaches, or by chance. Among these was the *tisB/istR* system in *E. coli*, which also encodes a toxin induced by the SOS response. The bicistronic *tisAB* locus encodes TisB (*toxicity induced by SOS*), a small peptide toxic to the cells in the absence of *istR* (*inhibitor of SOS-induced toxicity by RNA*) (28). Unlike SIB RNAs, this antitoxic sRNA is not *cis*-encoded. However, as is the case with *trans*-encoded sRNAs, *istR* has a 23 nucleotide region of complementarity with the *tisAB* mRNA, including the Shine-Dalgarno sequence and the start codon of *tisA*. By binding the mRNA, *istR* prevents ribosome loading and promotes an RNase III-mediated cleavage, rendering the mRNA translationally inactive (28). It has been suggested that this system could benefit the cells by arresting growth so that cells can work on DNA damage repair before cell division (28). Additionally, a decrease in the number of persister cells after

treatment with a DNA damaging antibiotic was observed in the absence of the *tisAB/istR* locus. These results suggest that TisB toxin plays a role in bacterial persister cell formation (29).

Similar to *istR*, the antitoxic sRNA OhsC (*oppression of hydrophobic ORF by sRNA*) is encoded divergently in the same region as the toxin ShoB (*short hydrophobic ORF*). As a result, it shares a limited region of complementarity (19 nucleotides) with the 5' UTR of toxin mRNA. ShoB overexpression reduces membrane potential, as does IbsC overexpression (25). However, the biological function of this TA has yet to be determined.

A very unique pair of Type I systems were identified recently by toxin similarity searches. In the Zor-Orz locus, two Zor (*Z-protein often repeated*) toxins with extensive sequence similarity are encoded in tandem (30). The antitoxin sRNAs, which were identified using RNA folding algorithms, are divergently encoded from their respective toxins but have perfect complementarity with a 20 nucleotide region at the 5'UTR of the toxin genes. Interestingly, the toxin and the antitoxin genes share their -35 promoter elements (30). This promoter overlap could potentially regulate the expression of the toxin gene by RNA polymerase competition. It should be noted that these TA loci are present in enterohemorrhagic *E.coli*, but not in the *E.coli* laboratory strain MG1655 (30).

Type I toxin-antitoxin systems in Gram-positive bacteria

Several Type I toxin-antitoxin systems have also been described in Gram-positive bacteria. Interestingly, while in Gram-negative bacteria the antitoxin sRNAs target the 5' of the toxin mRNA, in Gram-positive organisms, the sRNAs target the 3' of the toxin

transcript (31). The reason for the differences in target binding is not well understood. However, it has been speculated that 5' to 3' exoribonucleases present in these organisms might play role in gene expression, a feature not present in *E. coli*. A few other distinct characteristics of Gram-positive TA systems will also be briefly discussed.

The RNAI-RNAII system encoded by the *par* locus was the first Gram-positive Type I TA to be characterized and it was discovered on plasmid pAD1 of *Enterococcus faecalis* (32). The toxin Fst (*faecalis* plasmid-stabilizing toxin) is encoded by RNAI. RNAII is convergently transcribed and shares a terminator with the RNAI transcript. The two RNAs also share two direct repeat sequences located at their 5' ends, which in the case of *fst*, flank the translation initiation signals. According to Greenfield *et al.* (32), the interaction between the sRNA and the toxin mRNA is initiated by the shared bidirectional terminator sequences followed by an interaction between the direct repeats which are transcribed in opposite directions. This interaction prevents *fst* translation by blocking the ribosome binding site. Systems homologous to *fst* have also been found in several bacterial genomes (33).

More than fourteen chromosomal Type I TA modules have been identified in *Bacillus* and four toxin families have been proposed (31). In fact, these systems seem to be far more abundant than Type II toxin-antitoxin modules in this organism. The first chromosomal Type I TA system described was *txpA-ratA* (34). Like in the RNAI-RNAII system, the *txpA* (*toxic peptide A*) and *ratA* (*RNA antitoxin A*) are organized in a convergent orientation and they share an approximately 120 nucleotide region of complementarity at their 3' ends. Regulation by RatA is initiated by an interaction

between its transcription terminator loop and the stem-loop 6 of *txpA*. This kissing complex allows the formation of a more extensive duplex, which gets degraded by RNase III (35).

The YonT family found in the *SPβ* prophage differs from other toxins because it is transcribed as part of a three-gene operon and the antitoxin sRNA has complementarity to the 3' of *yonT*, as well as the 5' end of the downstream gene. It is not known if the sRNA also plays a role in the expression of the genes cotranscribed with the toxin. However, the *yonT/as-YonT* duplex gets degraded by RNase III (35).

An RNase III-independent Type I toxin-antitoxin system has also been described in *Bacillus*. The *bsrH* locus is located in the same intergenic region as *txpA* in the *skin* prophage. In this case, data suggest that the toxin and the antitoxin RNAs are degraded by exonucleases, including RNase PH and RNase R (35). Further studies are needed to dissect this new gene expression regulation pathway.

sRNA-mediated regulation of non-toxin genes expression

Before their characterization as antitoxins, some sRNAs were known to regulate gene expression by base-pairing to target mRNAs. For example, MicF, the first chromosomally encoded regulatory sRNA described, prevents the translation of the outer membrane porin OmpF by binding to its mRNA (36). Although the toxin and the antitoxin are encoded in *trans*, they share a region of complementarity of approximately 20 nucleotides. MicF binds to the translation initiation region the *ompF* mRNA, which includes the Shine-Dalgarno sequence and the start codon, and inhibits 30S ribosome loading. This translational inhibition is independent of RNase III activity and Hfq (37).

sRNAs can also regulate gene expression by inducing mRNA degradation. The sRNA RyhB, a regulator of iron metabolism, can base pair to the ribosome binding site and trigger the degradation of at least eighteen target mRNAs (38). The degradation of these mRNAs is dependent on the RNase E degradosome and Hfq (39).

Not all sRNAs have a negative regulatory effect on their targets. The acid stress regulatory circuit is an example of a positive regulation by a sRNA. The *cis*-encoded sRNA GadY binds to the intergenic region of the *gadX-gadW* bicistronic transcript (40). The duplex is processed by RNase III and other unidentified enzyme(s), and, as a result, *gadX* and *gadW* transcripts, which encode for transcriptional regulators of the glutamate-dependent acid response, become more stable (40,41).

Type II toxin-antitoxin systems

Like Type I toxin-antitoxin systems, Type II TA systems were first identified in bacterial plasmids. They generally consist of an operon encoding a labile antitoxin protein upstream of a more stable toxic peptide of around 100 amino acids (42). Type II toxin-antitoxin systems rely on the differential stability of the toxin and the antitoxin peptides. When the TA module is not transmitted to the daughter cells, the toxin and antitoxin are no longer expressed. As a result, the antitoxin pool is not replenished, the unstable antitoxic peptide is quickly degraded, while the stable toxic protein is released and free to act on its cellular target [reviewed in (4)]. Toxins found in TA systems have been shown to target essential cellular functions such as DNA replication and translation, with the latter being the most common target. Out of the 34 TA systems identified in *E.coli*, 14 have been well characterized, and with 11 of them the toxin protein has endoribonuclease

activity (3). However, with the use of bioinformatics, new toxin-antitoxin systems are constantly being discovered and novel families are likely to emerge (43).

In addition to the protein nature of the antitoxin, Type II toxin-antitoxin systems share several other common features. As aforementioned, the toxin and the antitoxin are co-expressed from an operon, where the antitoxin gene is normally located upstream of the toxin. To date, only three TA loci have been found in which the toxin is located upstream of the antitoxin (44,45). Furthermore, all the Type II antitoxins characterized thus far are unstable due to proteolysis by either Clp or Lon proteases. Type II toxin-antitoxin systems also share a mechanism of transcriptional autoregulation. The antitoxin proteins by themselves, or in conjunction with the toxins, negatively regulate transcription of their respective operons (46), with the exception of the zeta-epsilon TA system where the autoregulation is mediated by a third element of the system (47). The ten Type II toxin-antitoxin families will be briefly described below.

Type II toxin families that affect DNA replication

Type II systems are currently classified into ten families based on toxin sequence homology. The first Type II toxin-antitoxin system identified and founder of this class of toxin family was discovered in the F plasmid. *ccd* was originally described as a cellular mechanism that coupled cell division to plasmid proliferation by preventing cell division (48). However, further analysis revealed that CcdB (control of cell death) is involved in plasmid maintenance via post-segregational killing. CcdB is a toxin that disrupts DNA replication by binding the GyrA subunit of DNA gyrase and inhibiting the DNA re-ligation step, which indirectly leads to double-stranded DNA breaks (49). CcdA can bind

to CcdB and reverse its toxic effect by a process that has been termed rejuvenation (50,51). This TA system has been found only in Gram-negative bacteria and several chromosomal homologues have been identified (52).

Similarly to CcdB, the ParE toxin of the *parDE* TA system found in the plasmid RK2 causes DNA double-stranded breaks by poisoning DNA gyrase (53). However, these two toxin peptides are unrelated and, although the mechanisms of action of ParE is still not well defined, evidence suggests that ParE and CcdB have a different effect on DNA gyrase (54). Interestingly, *parDE* homologues found in chromosome II of *Vibrio cholerae* seem to play a role in ensuring the inheritance of the chromosome similar to the role *parDE* plays in plasmid maintenance (55).

Type II toxin families that affect translation without targeting mRNA

Another family of Type II toxin-antitoxins is found in the prophage P1. Doc (*death on curing*) is a toxin that, instead of poisoning DNA gyrase, inhibits translation elongation by binding to the 30S ribosomal subunit (56). Its toxic effect is inhibited by the Phd (*prevention of host death*) antitoxin (57). Structural studies suggest that Phd prevents Doc from binding ribosomes by forming a big complex and causing steric hindrance (58). This type of TA system is not very abundant, but it has been found in cassettes of chromosomal integrons in *Vibrio* (59).

HipA was first identified in *E. coli* by its role in *higher persistence*, a dormant state in which a subpopulation of bacterial cells neither grow nor die in the presence of antibiotics (60). Structural studies revealed that HipA shares similarities with eukaryotic serine/threonine protein kinases. It can phosphorylate the elongation factor EF-Tu,

therefore inhibiting protein synthesis (61). Its kinase activity is inhibited by HipB binding (61). The chromosomal HipBA module is one of the two TA systems known to date where the toxin is encoded upstream of its antitoxin (44).

Type II toxin family that affects peptidoglycan synthesis

The epsilon-zeta (PezAT) toxin-antitoxin family was first identified in a streptococcal plasmid and has been found only in Gram-positive bacteria (62). This system is unique in the Type II TA families because the toxin-antitoxin protein complex does not participate in the transcriptional regulation of the operon like in other toxin-antitoxin complexes. Autoregulation is mediated by omega, a third component of the TA system (63). Like HipA, PezT is a kinase. However, it is the first toxin known to target and inhibit bacterial peptidoglycan synthesis by phosphorylating a peptidoglycan precursor (64).

Type II toxin families that target mRNA

Ribosome-independent RNA interferases

A few years after CcdAB toxin-antitoxin system was discovered in the F plasmid, the ParD (Kis/Kid) TA system was found in the plasmid R1. The *parD* locus encodes the toxin Kid (*killing determinant*) and the antitoxin Kis (*killing suppressor*) (65). The Kis/Kid system is homologous to the PemIK (*plasmid emergency maintenance*) TA system of R100 (66,67). PemK has been shown to cleave mRNAs at UAH sequences (where H can be either a C, an A, or a U) (68,69). Toxins with the ability to cleave mRNAs at specific sequences, leading to the general inhibition of protein synthesis, have been termed mRNA-interferases [reviewed in (70)].

The first chromosomal TA systems identified were two *pemK* homologues, *chpA* and *chpB*. The *chpA* locus encodes for ChpAI (MazE) and ChpAK (MazF) (71). MazF, also an RNA intereferase, cleaves mRNAs at ACA sequences in ribosome-free mRNAs (72,73). Similarly, ChpBK can cleave mRNA at ACA, ACG, or ACU sequences (74). Both proteins are therefore classified as a ribosome-independent interferases (3). MazF is the best-characterized bacterial toxin thus far. PemK, Kid, and ChpBK are all part of the MazEF toxin family.

The MazEF TA module in *E.coli* is part of the *rel* operon, with the *relA* gene located upstream and *mazG* downstream (75,76). *relA* encodes for an enzyme required for guanosine 3',5'-bispyrophosphate (ppGpp) synthesis, a major regulator of the stringent response. Its expression is induced in response to amino acid starvation. ppGpp was also shown to inhibit transcription of the *mazEF* operon (75). MazG encodes a nucleotide pyrophosphohydrolase that can lower the levels of ppGpp in the cell and therefore inhibit the induction of the stringent response. Interestingly, the enzymatic activity of MazG is greatly inhibited in the presence of MazEF. Gross *et al.* (77) proposed a model where MazG also plays a role in MazEF-mediated cell death. As a result of nutritional stress, ppGpp levels go up, inhibiting transcription of the *mazEF* operon. The remaining MazE proteins are degraded by proteases, freeing MazF from its antitoxin. In turn, degradation of MazE releases the repression the MazEF complex has on MazG activity, allowing MazG to deplete the pool of ppGpp, shutting down the stringent response and allowing the new transcription of the MazEF operon (77).

In addition to amino acid starvation, MazF has been shown to be activated by antibiotics that inhibit transcription and/or translation, such as chloramphenicol and rifampicin, as well as DNA damaging agents including nalidixic acid and mitomycin C (78,79).

MazEF toxicity depends on the presence of EDF (*extracellular death factor*), a small, quorum-sensing peptide produced in dense cultures (80). It was recently shown that EDF binds to MazF and ChpBK and enhances their endoribonucleolytic activities *in vitro*, adding to the complexity of *mazEF* regulation (81).

It has been proposed that MazEF mediates a programmed cell death (PCD) pathway in response to stress, but there is still some controversy about the reproducibility of results (80). It has been suggested that MazF activation has a bacteriostatic effect on the cell population rather than bacteriocidal (82).

However, a role for MazF in the programmed cell death of *Myxococcus* has been established (6). *Myxococcus* is a Gram-negative bacterium that forms fruiting bodies upon nutrient starvation. This process is severely affected in the absence of MazF. Unlike every other Type II TA system, no antitoxin gene is cotranscribed with *mazF* in this organism. Instead, MazF is kept inactive under normal growth conditions by MrpC, which is encoded elsewhere in the chromosome (6).

Another ribosome-independent Type II toxin-antitoxin family has been described in the *E.coli* chromosome. HicA encodes the toxin of the chromosomal HicAB toxin-antitoxin family and its located upstream of the antitoxin (83). The locus was first identified in *Haemophilus influenzae* (*hif*) and was called *hic* for *hif* contiguous (84). In the

absence of HicB, HicA inhibits translation by cleaving mRNA independently of translation. It can also cleave tmRNA. However, no consensus cleavage sequence has been identified (85).

YgiT, also known as MqsR (*motility quorum sensor regulator*), is the only ribosome-independent mRNA interferase known to date to belong to RelE family of toxins (described below) (45). It cleaves mRNAs at GCU sites (86). Upon MqsR activation, which is induced during biofilm formation, most of the cellular mRNAs are susceptible to MqsR degradation. Interestingly, 14 of the *E.coli* ORFs lack GCU sequences, making them resistant to MqsR activity. Six of these 14 genes are also induced upon biofilm formation (86). Their resistance to MqsR cleavage ensures their expression at a critical moment for the bacterial population.

Ribosome-dependent RNA interferases

The most studied ribosome-dependent interferase is RelE. The RelBE locus was first described as a toxin-antitoxin system in the *E.coli* chromosome in the late 90's (87). However, the *relB* gene had been identified 20 years earlier due to the delayed relaxed response exhibited by *relB* mutants after amino acid starvation (88,89). RelE inhibits global protein synthesis by cleaving mRNAs in a ribosome-dependent manner (90). It cleaves mRNAs at the A site of the ribosome, between the second and third nucleotides. The RelB antitoxin binds to RelE and reverses the inhibition of translation (91). Most of the chromosomally encoded mRNA interferases in *E.coli* belong to the RelE superfamily. Additionally, homologues of the RelBE TA systems have also been found in plasmids (92).

The toxins YgjN/HigB (*host inhibition of growth*), YoeB, YafQ, and YafO, all members of the RelE TA family, have been characterized as ribosome-dependent mRNA interferases (45). HigB is one of only three TA systems known to date where the toxin is encoded upstream of the antitoxin. Surprisingly, although YoeB interacts with the 50S ribosomal subunit and cleaves mRNAs at the A site, its toxic effect seems to be associated with preventing the formation of the translation initiation complex and not with its endoribonuclease activity (93). YafQ associates with the 50S ribosomal subunit of the 70S ribosome and cleaves mRNAs at in-frame AAA (lysine) codons followed by a purine residue (94). YafO also associates with the 50S subunit of 70S ribosomes, but it cleaves mRNAs outside of the ribosome-protected region, 11-13 bases downstream of the initiation codon (95). In addition, the *YafNO* toxin-antitoxin system is the only Type II TA known to date to be regulated by the SOS DNA damage response (96).

New type of interferase - tRNAse

Of the TA loci identified up to date, the VapBC (*virulence associated protein*) family is the most abundant (97). VapC toxins are site-specific endoribonucleases that inhibit translation by cleaving tRNA^{fMet}, the initiator tRNA (98). Because of their activity, VapC toxins have been termed tRNAases. However, different RNA targets have been identified in different organisms (99). Their bacteriostatic effect can be reversed by the addition of the antitoxin VapB or fMet-tRNA^{fMet} (98). In addition, VapC activation leads to YoeB-mediated mRNA cleavage (97). This cross-activation between TA systems was also reported for *phd-doc* and *mazEF*, where plasmid loss leads to Doc activation and

the global inhibition of translation. As a result, MazE levels drop and MazF is free to act on mRNAs (100).

This review has highlighted the abundance of toxin-antitoxin systems and their various modes of action. As techniques improve, the discovery and thorough characterization of new and existing TA systems will help fill in the gaps about their biological roles and importance.

My dissertation research has focused on expanding our understanding of the role of ribonucleases in toxin-antitoxin systems in *E.coli*. Chapter 2 provides a broader look at the processing of the *cis*-encoded Type I toxin-antitoxin system SibC/*ibsC* by ribonucleases. We separated target-dependent and target-independent events to get a better understanding of the sRNA biology and how it regulates *ibsC* expression. We have also evaluated the involvement of the RNA chaperone Hfq in the stability of SibC and examined its involvement in the regulation of *ibsC*. Chapter 3 examines the role of the Type II ribosome-dependent RNA interferase MazF in general message decay in *E.coli*. Our data, surprisingly, suggests an indirect role for MazG in message decay likely related to the misregulation of stringent response.

REFERENCES

1. Gerdes, K., Larsen, J.E. and Molin, S. (1985) Stable inheritance of plasmid R1 requires two different loci. *J. Bacteriol.*, 161, 292-298.
2. Gerdes, K., Rasmussen, P.B. and Molin, S. (1986) Unique type of plasmid maintenance function: postsegregational killing of plasmid-free cells. *Proc. Natl. Acad. Sci. U S A*, 83, 3116-3120.
3. Yamaguchi, Y., Park, J.H. and Inouye, M. (2011) Toxin-antitoxin systems in bacteria and archaea. *Annu. Rev. Genet.*, 45, 61-79.
4. Gerdes, K., Christensen, S.K. and Lobner-Olesen, A. (2005) Prokaryotic toxin-antitoxin stress response loci. *Nat. Rev.*, 3, 371-382.
5. Buts, L., Lah, J., Dao-Thi, M.H., Wyns, L. and Loris, R. (2005) Toxin-antitoxin modules as bacterial metabolic stress managers. *Trends Biochem. Sci.*, 30, 672-679.
6. Nariya, H. and Inouye, M. (2008) MazF, an mRNA interferase, mediates programmed cell death during multicellular *Myxococcus* development. *Cell*, 132, 55-66.
7. Blower, T.R., Fineran, P.C., Johnson, M.J., Toth, I.K., Humphreys, D.P. and Salmond, G.P. (2009) Mutagenesis and functional characterization of the RNA and protein components of the toxIN abortive infection and toxin-antitoxin locus of *Erwinia*. *J. Bacteriol.*, 191, 6029-6039.
8. Blower, T.R., Pei, X.Y., Short, F.L., Fineran, P.C., Humphreys, D.P., Luisi, B.F. and Salmond, G.P. (2011) A processed noncoding RNA regulates an altruistic bacterial antiviral system. *Nat. Struct. Mol. Biol.*, 18, 185-190.

9. Fineran, P.C., Blower, T.R., Foulds, I.J., Humphreys, D.P., Lilley, K.S. and Salmond, G.P. (2009) The phage abortive infection system, ToxIN, functions as a protein-RNA toxin-antitoxin pair. *Proc. Natl. Acad. Sci. U S A*, 106, 894-899.
10. Blower, T.R., Short, F.L., Rao, F., Mizuguchi, K., Pei, X.Y., Fineran, P.C., Luisi, B.F. and Salmond, G.P. (2012) Identification and classification of bacterial Type III toxin-antitoxin systems encoded in chromosomal and plasmid genomes. *Nucleic Acids Res.*, 40, 6158-6173.
11. Tan, Q., Awano, N. and Inouye, M. (2011) YeeV is an *Escherichia coli* toxin that inhibits cell division by targeting the cytoskeleton proteins, FtsZ and MreB. *Mol. Microbiol.*, 79, 109-118.
12. Brown, J.M. and Shaw, K.J. (2003) A novel family of *Escherichia coli* toxin-antitoxin gene pairs. *J. Bacteriol.*, 185, 6600-6608.
13. Masuda, H., Tan, Q., Awano, N., Yamaguchi, Y. and Inouye, M. (2012) A novel membrane-bound toxin for cell division, CptA (YgfX), inhibits polymerization of cytoskeleton proteins, FtsZ and MreB, in *Escherichia coli*. *FEMS Microbiol. Lett.*, 328, 174-181.
14. Wang, X., Lord, D.M., Cheng, H.Y., Osbourne, D.O., Hong, S.H., Sanchez-Torres, V., Quiroga, C., Zheng, K., Herrmann, T., Peti, W. *et al.* (2012) A new type V toxin-antitoxin system where mRNA for toxin GhoT is cleaved by antitoxin GhoS. *Nat. Chem. Biol.*, 8, 855-861.
15. Kawano, M. (2012) Divergently overlapping *cis*-encoded antisense RNA regulating toxin-antitoxin systems from *E. coli*: *hok/sok*, *ldr/rdl*, *symE/symR*. *RNA Biol.*, 9, 1520-1527.

16. Fozo, E.M., Hemm, M.R. and Storz, G. (2008) Small toxic proteins and the antisense RNAs that repress them. *Microbiol. Mol. Biol. Rev.*, 72, 579-589
17. Gottesman, S. (2005) Micros for microbes: non-coding regulatory RNAs in bacteria. *Trends Genet.*, 21, 399-404.
18. Thisted, T. and Gerdes, K. (1992) Mechanism of post-segregational killing by the hok/sok system of plasmid R1. Sok antisense RNA regulates *hok* gene expression indirectly through the overlapping *mok* gene. *J. Mol. Biol.*, 223, 41-54.
19. Gerdes, K., Nielsen, A., Thorsted, P. and Wagner, E.G. (1992) Mechanism of killer gene activation. Antisense RNA-dependent RNase III cleavage ensures rapid turn-over of the stable *hok*, *srnB* and *pndA* effector messenger RNAs. *J. Mol. Biol.*, 226, 637-649.
20. Loh, S.M., Cram, D.S. and Skurray, R.A. (1988) Nucleotide sequence and transcriptional analysis of a third function (Flm) involved in F-plasmid maintenance. *Gene*, 66, 259-268.
21. Ohnishi, Y., Iguma, H., Ono, T., Nagaishi, H. and Clark, A.J. (1977) Genetic mapping of the F plasmid gene that promotes degradation of stable ribonucleic acid in *Escherichia coli*. *J. Bacteriol.*, 132, 784-789.
22. Pedersen, K. and Gerdes, K. (1999) Multiple hok genes on the chromosome of *Escherichia coli*. *Mol. Microbiol.*, 32, 1090-1102.
23. Gerdes, K. and Wagner, E.G. (2007) RNA antitoxins. *Curr. Opin. Microbiol.*, 10, 117-124.
24. Rudd, K.E. (1999) Novel intergenic repeats of *Escherichia coli* K-12. *Res. Microbiol.*, 150, 653-664.

25. Fozo, E.M., Kawano, M., Fontaine, F., Kaya, Y., Mendieta, K.S., Jones, K.L., Ocampo, A., Rudd, K.E. and Storz, G. (2008) Repression of small toxic protein synthesis by the Sib and OhsC small RNAs. *Mol. Microbiol.*, 70, 1076-1093.
26. Kawano, M., Aravind, L. and Storz, G. (2007) An antisense RNA controls synthesis of an SOS-induced toxin evolved from an antitoxin. *Mol. Microbiol.*, 64, 738-754.
27. Fernandez De Henestrosa, A.R., Ogi, T., Aoyagi, S., Chafin, D., Hayes, J.J., Ohmori, H. and Woodgate, R. (2000) Identification of additional genes belonging to the LexA regulon in *Escherichia coli*. *Mol. Microbiol.*, 35, 1560-1572.
28. Vogel, J., Argaman, L., Wagner, E.G. and Altuvia, S. (2004) The small RNA IstR inhibits synthesis of an SOS-induced toxic peptide. *Curr. Biol.*, 14, 2271-2276.
29. Dorr, T., Vulic, M. and Lewis, K. Ciprofloxacin causes persister formation by inducing the TisB toxin in *Escherichia coli*. *PLoS Biol.*, 8, e1000317.
30. Fozo, E.M., Makarova, K.S., Shabalina, S.A., Yutin, N., Koonin, E.V. and Storz, G. (2010) Abundance of type I toxin-antitoxin systems in bacteria: searches for new candidates and discovery of novel families. *Nucleic Acids Res.*, 38, 3743-3759.
31. Durand, S., Jahn, N., Condon, C. and Brantl, S. (2012) Type I toxin-antitoxin systems in *Bacillus subtilis*. *RNA Biol.*, 9, 1491-1497.
32. Greenfield, T.J., Franch, T., Gerdes, K. and Weaver, K.E. (2001) Antisense RNA regulation of the par post-segregational killing system: structural analysis and mechanism of binding of the antisense RNA, RNAII and its target, RNAI. *Mol. Microbiol.*, 42, 527-537.

33. Weaver, K.E., Reddy, S.G., Brinkman, C.L., Patel, S., Bayles, K.W. and Endres, J.L. (2009) Identification and characterization of a family of toxin-antitoxin systems related to the *Enterococcus faecalis* plasmid pAD1 par addiction module. *Microbiol.*, 155, 2930-2940.
34. Silvaggi, J.M., Perkins, J.B. and Losick, R. (2005) Small untranslated RNA antitoxin in *Bacillus subtilis*. *J. Bacteriol.*, 187, 6641-6650.
35. Durand, S., Gilet, L. and Condon, C. (2012) The essential function of *B. subtilis* RNase III is to silence foreign toxin genes. *PLoS Genet.*, 8, e1003181.
36. Mizuno, T., Chou, M.Y. and Inouye, M. (1984) A unique mechanism regulating gene expression: translational inhibition by a complementary RNA transcript (micRNA). *Proc. Natl. Acad. Sci. U S A*, 81, 1966-1970.
37. Urban, J.H. and Vogel, J. (2007) Translational control and target recognition by *Escherichia coli* small RNAs in vivo. *Nucleic Acids Res.*, 35, 1018-1037.
38. Masse, E., Vanderpool, C.K. and Gottesman, S. (2005) Effect of RyhB small RNA on global iron use in *Escherichia coli*. *J. Bacteriol.*, 187, 6962-6971.
39. Prevost, K., Desnoyers, G., Jacques, J.F., Lavoie, F. and Masse, E. (2011) Small RNA-induced mRNA degradation achieved through both translation block and activated cleavage. *Genes Dev.*, 25, 385-396.
40. Opdyke, J.A., Kang, J.G. and Storz, G. (2004) GadY, a small-RNA regulator of acid response genes in *Escherichia coli*. *J. Bacteriol.*, 186, 6698-6705.
41. Opdyke, J.A., Fozo, E.M., Hemm, M.R. and Storz, G. (2011) RNase III participates in GadY-dependent cleavage of the *gadX-gadW* mRNA. *J. Mol. Biol.*, 406, 29-43.

42. Gerdes, K. (2000) Toxin-antitoxin modules may regulate synthesis of macromolecules during nutritional stress. *J. Bacteriol.*, 182, 561-572.
43. Leplae, R., Geeraerts, D., Hallez, R., Guglielmini, J., Dreze, P. and Van Melderen, L. (2011) Diversity of bacterial type II toxin-antitoxin systems: a comprehensive search and functional analysis of novel families. *Nucleic Acids Res.*, 39, 5513-5525.
44. Black, D.S., Kelly, A.J., Mardis, M.J. and Moyed, H.S. (1991) Structure and organization of *hip*, an operon that affects lethality due to inhibition of peptidoglycan or DNA synthesis. *J. Bacteriol.*, 173, 5732-5739.
45. Christensen-Dalsgaard, M., Jorgensen, M.G. and Gerdes, K. Three new RelE-homologous mRNA interferases of *Escherichia coli* differentially induced by environmental stresses. *Mol. Microbiol.*, 75, 333-348.
46. Jensen, R.B. and Gerdes, K. (1995) Programmed cell death in bacteria: proteic plasmid stabilization systems. *Mol. Microbiol.*, 17, 205-210.
47. Zielenkiewicz, U. and Ceglowski, P. (2005) The toxin-antitoxin system of the streptococcal plasmid pSM19035. *J. Bacteriol.*, 187, 6094-6105.
48. Ogura, T. and Hiraaga, S. (1983) Mini-F plasmid genes that couple host cell division to plasmid proliferation. *Proc. Natl. Acad. Sci. U S A*, 80, 4784-4788.
49. Bernard, P. and Couturier, M. (1992) Cell killing by the F plasmid CcdB protein involves poisoning of DNA-topoisomerase II complexes. *J. Mol. Biol.*, 226, 735-745.
50. Tam, J.E. and Kline, B.C. (1989) The F plasmid *ccd* autorepressor is a complex of CcdA and CcdB proteins. *Mol. Gen. Genet.*, 219, 26-32.

51. Maki, S., Takiguchi, S., Horiuchi, T., Sekimizu, K. and Miki, T. (1996) Partner switching mechanisms in inactivation and rejuvenation of *Escherichia coli* DNA gyrase by F plasmid proteins LetD (CcdB) and LetA (CcdA). *J. Mol. Biol.*, 256, 473-482.
52. Syed, M.A. and Levesque, C.M. (2012) Chromosomal bacterial type II toxin-antitoxin systems. *Can. J. Microbiol.*, 58, 553-562.
53. Jiang, Y., Pogliano, J., Helinski, D.R. and Konieczny, I. (2002) ParE toxin encoded by the broad-host-range plasmid RK2 is an inhibitor of *Escherichia coli* gyrase. *Mol. Microbiol.*, 44, 971-979.
54. Yuan, J., Sterckx, Y., Mitchenall, L.A., Maxwell, A., Loris, R. and Waldor, M.K. (2010) *Vibrio cholerae* ParE2 poisons DNA gyrase via a mechanism distinct from other gyrase inhibitors. *J. Biol. Chem.*, 285, 40397-40408.
55. Yuan, J., Yamaichi, Y. and Waldor, M.K. (2011) The three *Vibrio cholerae* chromosome II-encoded ParE toxins degrade chromosome I following loss of chromosome II. *J. Bacteriol.*, 193, 611-619.
56. Liu, M., Zhang, Y., Inouye, M. and Woychik, N.A. (2008) Bacterial addiction module toxin Doc inhibits translation elongation through its association with the 30S ribosomal subunit. *Proc. Natl. Acad. Sci. U S A*, 105, 5885-5890.
57. Lehnerr, H., Maguin, E., Jafri, S. and Yarmolinsky, M.B. (1993) Plasmid addiction genes of bacteriophage P1: doc, which causes cell death on curing of prophage, and phd, which prevents host death when prophage is retained. *J. Mol. Biol.*, 233, 414-428.

58. Arbing, M.A., Handelman, S.K., Kuzin, A.P., Verdon, G., Wang, C., Su, M., Rothenbacher, F.P., Abashidze, M., Liu, M., Hurley, J.M. *et al.* (2010) Crystal structures of Phd-Doc, HigA, and YeeU establish multiple evolutionary links between microbial growth-regulating toxin-antitoxin systems. *Structure*, 18, 996-1010.
59. Rowe-Magnus, D.A., Guerout, A.M., Biskri, L., Bouige, P. and Mazel, D. (2003) Comparative analysis of superintegrons: engineering extensive genetic diversity in the Vibrionaceae. *Genome Res.*, 13, 428-442.
60. Moyed, H.S. and Bertrand, K.P. (1983) hipA, a newly recognized gene of *Escherichia coli* K-12 that affects frequency of persistence after inhibition of murein synthesis. *J. Bacteriol.*, 155, 768-775.
61. Schumacher, M.A., Piro, K.M., Xu, W., Hansen, S., Lewis, K. and Brennan, R.G. (2009) Molecular mechanisms of HipA-mediated multidrug tolerance and its neutralization by HipB. *Science*, 323, 396-401.
62. Ceglowski, P., Boitsov, A., Karamyan, N., Chai, S. and Alonso, J.C. (1993) Characterization of the effectors required for stable inheritance of *Streptococcus pyogenes* pSM19035-derived plasmids in *Bacillus subtilis*. *Mol. Gen. Genet.*, 241, 579-585.
63. de la Hoz, A.B., Ayora, S., Sitkiewicz, I., Fernandez, S., Pankiewicz, R., Alonso, J.C. and Ceglowski, P. (2000) Plasmid copy-number control and better-than-random segregation genes of pSM19035 share a common regulator. *Proc. Natl. Acad. Sci. U S A*, 97, 728-733.

64. Mutschler, H., Gebhardt, M., Shoeman, R.L. and Meinhart, A. (2011) A novel mechanism of programmed cell death in bacteria by toxin-antitoxin systems corrupts peptidoglycan synthesis. *PLoS Biol.*, 9, e1001033.
65. Bravo, A., de Torriontegui, G. and Diaz, R. (1987) Identification of components of a new stability system of plasmid R1, ParD, that is close to the origin of replication of this plasmid. *Mol. Gen. Genet.*, 210, 101-110.
66. Bravo, A., Ortega, S., de Torriontegui, G. and Diaz, R. (1988) Killing of *Escherichia coli* cells modulated by components of the stability system ParD of plasmid R1. *Mol. Gen. Genet.*, 215, 146-151.
67. Tsuchimoto, S., Ohtsubo, H. and Ohtsubo, E. (1988) Two genes, pemK and pemI, responsible for stable maintenance of resistance plasmid R100. *J. Bacteriol.*, 170, 1461-1466.
68. Zhang, J., Zhang, Y., Zhu, L., Suzuki, M. and Inouye, M. (2004) Interference of mRNA function by sequence-specific endoribonuclease PemK. *J. Biol. Chem.*, 279, 20678-20684.
69. Munoz-Gomez, A.J., Lemonnier, M., Santos-Sierra, S., Berzal-Herranz, A. and Diaz-Orejas, R. (2005) RNase/anti-RNase activities of the bacterial parD toxin-antitoxin system. *J. Bacteriol.*, 187, 3151-3157.
70. Inouye, M. (2006) The discovery of mRNA interferases: implication in bacterial physiology and application to biotechnology. *J. Cell. Physiol.*, 209, 670-676.
71. Masuda, Y., Miyakawa, K., Nishimura, Y. and Ohtsubo, E. (1993) *chpA* and *chpB*, *Escherichia coli* chromosomal homologs of the *pem* locus responsible for stable maintenance of plasmid R100. *J. Bacteriol.*, 175, 6850-6856.

72. Zhang, Y., Zhang, J., Hoeflich, K.P., Ikura, M., Qing, G. and Inouye, M. (2003) MazF cleaves cellular mRNAs specifically at ACA to block protein synthesis in *Escherichia coli*. *Mol. Cell*, 12, 913-923.
73. Christensen, S.K., Mikkelsen, M., Pedersen, K. and Gerdes, K. (2001) RelE, a global inhibitor of translation, is activated during nutritional stress. *Proc. Natl. Acad. Sci. U S A*, 98, 14328-14333.
74. Zhang, Y., Zhu, L., Zhang, J. and Inouye, M. (2005) Characterization of ChpBK, an mRNA interferase from *Escherichia coli*. *J. Biol. Chem.*, 280, 26080-26088.
75. Aizenman, E., Engelberg-Kulka, H. and Glaser, G. (1996) An *Escherichia coli* chromosomal "addiction module" regulated by guanosine [corrected] 3',5'-bispyrophosphate: a model for programmed bacterial cell death. *Proc. Natl. Acad. Sci. U S A*, 93, 6059-6063.
76. Zhang, J. and Inouye, M. (2002) MazG, a nucleoside triphosphate pyrophosphohydrolase, interacts with Era, an essential GTPase in *Escherichia coli*. *J. Bacteriol.*, 184, 5323-5329.
77. Gross, M., Marianovsky, I. and Glaser, G. (2006) MazG -- a regulator of programmed cell death in *Escherichia coli*. *Mol. Microbiol.*, 59, 590-601.
78. Sat, B., Hazan, R., Fisher, T., Khaner, H., Glaser, G. and Engelberg-Kulka, H. (2001) Programmed cell death in *Escherichia coli*: some antibiotics can trigger mazEF lethality. *J. Bacteriol.*, 183, 2041-2045.
79. Hazan, R., Sat, B. and Engelberg-Kulka, H. (2004) *Escherichia coli* mazEF-mediated cell death is triggered by various stressful conditions. *J. Bacteriol.*, 186, 3663-3669.

80. Kolodkin-Gal, I., Hazan, R., Gaathon, A., Carmeli, S. and Engelberg-Kulka, H. (2007) A linear pentapeptide is a quorum-sensing factor required for mazEF-mediated cell death in *Escherichia coli*. *Science*, 318, 652-655.
81. Belitsky, M., Avshalom, H., Erental, A., Yelin, I., Kumar, S., London, N., Sperber, M., Schueler-Furman, O. and Engelberg-Kulka, H. (2011) The *Escherichia coli* extracellular death factor EDF induces the endoribonucleolytic activities of the toxins MazF and ChpBK. *Mol. Cell*, 41, 625-635.
82. Christensen, S.K., Pedersen, K., Hansen, F.G. and Gerdes, K. (2003) Toxin-antitoxin loci as stress-response-elements: ChpAK/MazF and ChpBK cleave translated RNAs and are counteracted by tmRNA. *J. Mol. Biol.*, 332, 809-819.
83. Makarova, K.S., Grishin, N.V. and Koonin, E.V. (2006) The HicAB cassette, a putative novel, RNA-targeting toxin-antitoxin system in archaea and bacteria. *Bioinformatics*, 22, 2581-2584.
84. Mhlanga-Mutangadura, T., Morlin, G., Smith, A.L., Eisenstark, A. and Golomb, M. (1998) Evolution of the major pilus gene cluster of *Haemophilus influenzae*. *J. Bacteriol.*, 180, 4693-4703.
85. Jorgensen, M.G., Pandey, D.P., Jaskolska, M. and Gerdes, K. (2009) HicA of *Escherichia coli* defines a novel family of translation-independent mRNA interferases in bacteria and archaea. *J. Bacteriol.*, 191, 1191-1199.
86. Yamaguchi, Y., Park, J.H. and Inouye, M. (2009) MqsR, a crucial regulator for quorum sensing and biofilm formation, is a GCU-specific mRNA interferase in *Escherichia coli*. *J. Biol. Chem.*, 284, 28746-28753.

87. Gotfredsen, M. and Gerdes, K. (1998) The *Escherichia coli* *relBE* genes belong to a new toxin-antitoxin gene family. *Mol. Microbiol.*, 29, 1065-1076.
88. Diderichsen, B., Fiil, N.P. and Lavalle, R. (1977) Genetics of the *relB* locus in *Escherichia coli*. *J. Bacteriol.*, 131, 30-33.
89. Mosteller, R.D. (1978) Evidence that glucose starvation-sensitive mutants are altered in the *relB* locus. *J. Bacteriol.*, 133, 1034-1037.
90. Pedersen, K., Zavialov, A.V., Pavlov, M.Y., Elf, J., Gerdes, K. and Ehrenberg, M. (2003) The bacterial toxin RelE displays codon-specific cleavage of mRNAs in the ribosomal A site. *Cell*, 112, 131-140.
91. Galvani, C., Terry, J. and Ishiguro, E.E. (2001) Purification of the RelB and RelE proteins of *Escherichia coli*: RelE binds to RelB and to ribosomes. *J. Bacteriol.*, 183, 2700-2703.
92. Gronlund, H. and Gerdes, K. (1999) Toxin-antitoxin systems homologous with *relBE* of *Escherichia coli* plasmid P307 are ubiquitous in prokaryotes. *J. Mol. Biol.*, 285, 1401-1415.
93. Zhang, Y. and Inouye, M. (2009) The inhibitory mechanism of protein synthesis by YoeB, an *Escherichia coli* toxin. *J. Biol. Chem.*, 284, 6627-6638.
94. Prysak, M.H., Mozdierz, C.J., Cook, A.M., Zhu, L., Zhang, Y., Inouye, M. and Woychik, N.A. (2009) Bacterial toxin YafQ is an endoribonuclease that associates with the ribosome and blocks translation elongation through sequence-specific and frame-dependent mRNA cleavage. *Mol. Microbiol.*, 71, 1071-1087.
95. Zhang, Y., Yamaguchi, Y. and Inouye, M. (2009) Characterization of YafO, an *Escherichia coli* toxin. *J. Biol. Chem.*, 284, 25522-25531.

96. Singletary, L.A., Gibson, J.L., Tanner, E.J., McKenzie, G.J., Lee, P.L., Gonzalez, C. and Rosenberg, S.M. (2009) An SOS-regulated type 2 toxin-antitoxin system. *J. Bacteriol.*, 191, 7456-7465.
97. Winther, K.S. and Gerdes, K. (2009) Ectopic production of VapCs from Enterobacteria inhibits translation and trans-activates YoeB mRNA interferase. *Mol. Microbiol.*, 72, 918-930.
98. Winther, K.S. and Gerdes, K. (2011) Enteric virulence associated protein VapC inhibits translation by cleavage of initiator tRNA. *Proc. Natl. Acad. Sci. U S A*, 108, 7403-7407.
99. Cook, G.M., Robson, J.R., Frampton, R.A., McKenzie, J., Przybilski, R., Fineran, P.C. and Arcus, V.L. (2013) Ribonucleases in bacterial toxin-antitoxin systems. *Biochim. Biophys. Acta* (in press).
100. Hazan, R., Sat, B., Reches, M. and Engelberg-Kulka, H. (2001) Postsegregational killing mediated by the P1 phage "addiction module" *phd-doc* requires the *Escherichia coli* programmed cell death system *mazEF*. *J. Bacteriol.*, 183, 2046-2050.

CHAPTER 2
ANALYSIS OF THE SIBC/*IBSC* TOXIN-ANTITOXIN SYSTEM IN *ESCHERICHIA*
*COLI*¹

¹ Roche Ríos, Marly I., Marshburn, Sarah E., and Kushner, Sidney R. To be submitted to *Nucleic Acids Research*.

ABSTRACT

The identification of small, regulatory RNAs (sRNAs) as important regulators of gene expression in prokaryotes has generated considerable interest, since they provide an important mechanism by which bacteria can rapidly adapt to changes in their environment. sRNAs bind to specific mRNAs and exert either a positive or negative effect on the stability or translatability of their targets. Their classification and, to some extent, their mechanism of action, are based on their location with regards to their respective target RNAs. The most common and best characterized bacterial sRNAs are transcribed from separate loci relative to their target(s). These *trans*-encoded sRNAs share only partial sequence homology with the mRNAs they regulate, and usually require RNase E and Hfq to mediate the destabilization of their target mRNAs.

In contrast, *cis*-encoded sRNAs arise from antisense transcription of their target genes and, as a result, share extensive regions of complete complementarity with their mRNA targets. These extensive duplexes are possible targets for RNase III cleavages, independent of an Hfq requirement. In this work, we have characterized the role of several endoribonucleases and Hfq in the biogenesis and decay of the *cis*-encoded sRNA SibC and its target *ibsC*. SibC/*ibsC* is a chromosomally encoded type I toxin-antitoxin system of unknown biological function, which is particularly interesting due to the fact that it belongs to the only family of sRNAs known to date to share complete sequence homology to their targets. Previous analysis revealed two SibC transcripts of approximately 140 and 110 nucleotides in length that share identical 5' termini, but differ at their 3' ends. Here we demonstrate that the shorter SibC transcript is not the result of processing of the SibC/*ibsC* duplex, as previously thought, since no differences in the

SibC profile were observed in the presence or absence of *ibsC* expression. We also show that RNase III, RNase E, RNase P and Hfq impact the rate of decay of SibC as assayed by chemical half-life determinations. Interestingly, RNase III seems to protect SibC from degradation by an unknown mechanism, suggesting a new role for RNase III in sRNA-mediated regulation of gene expression. We also show a role for Hfq in two aspects of the regulation of *ibsC* by SibC. It protects SibC from degradation by RNase E in a manner dependent on the C-terminal scaffold region of RNase E and it mediates the destabilization of the *ibsC* mRNA. Taken together these results expand the repertoire of roles for Hfq to include the regulation of gene expression mediated by *cis*-encoded sRNAs.

INTRODUCTION

Small, regulatory RNAs (sRNAs) are important biological regulators in prokaryotes, providing mechanisms by which bacteria can rapidly adapt to changes in their environment. They regulate processes such as plasmid replication, transposition, and gene expression by base pairing to their target RNAs [reviewed in (1)]. Upon binding, sRNA can either positively or negatively affect message stability or translatability, although negative regulation seems to be predominant in the regulatory circuits described thus far (2).

The first example of sRNA-mediated regulation of gene expression came from the analysis of MicF. MicF is a chromosomally encoded sRNA that binds to the 5' UTR of the outer membrane protein *ompF* and prevents its translation (3). Subsequently, sRNAs were also characterized as antitoxins in plasmid toxin-antitoxin systems (4).

Toxin-antitoxin (TA) modules consist of a stable toxin that, upon overexpression, leads to cell stasis or death, and a labile antitoxin that specifically inhibits its toxic effect. The unstable nature of the antitoxin ensures the inheritance of the plasmid. Cells that fail to inherit a plasmid containing the TA locus quickly lose the antitoxin, which allows the toxic proteins to kill the plasmid-free cells. This process is known as post-segregational killing (PSK) (4). PSK was first described on the R1 plasmid, where the *cis*-encoded sRNA Sok binds to the translational initiation region (TIR) at the 5' UTR of the *mok-hok* mRNA, prevents the translation of the Hok toxin, and leads to RNase III-mediated cleavage of the sRNA:mRNA duplex (4,5). Toxin-antitoxin systems like *hok/sok*, where the toxin inhibition is mediated by a sRNA that binds to the mRNA of the toxin protein,

are classified as Type I. Four additional types of TA systems (Types II-V) have been described where the inhibitory mechanisms are not mediated by the base pairing of sRNAs to the toxin-encoding mRNAs.

Small RNAs are classified according to their location with regards to their respective targets. *cis*-encoded sRNAs, such as Sok and GadY, arise from antisense transcription of protein-coding genes. As a result, the sRNAs and the target mRNAs share extensive regions of complementarity. Several mechanisms by which *cis*-encoded sRNAs regulate the expression of their respective target mRNAs have been partially characterized, and like the *hok/sok* system, most of them require RNase III activity. For example, GadY positively regulates *gadX* expression by binding to the *gadWX* mRNA. Upon GadY binding, cleavage of bicistronic transcript by RNase III and some other unidentified enzyme(s) results in the stabilization of the *gadX* mRNA (24). An undefined role for RNase E in the expression of GadY has also been described, suggesting a possible role for RNase E in GadY-mediated regulation of *gadX* (25). However, not every *cis*-encoded sRNA regulates gene expression via RNase III. SymR, a sRNA with complete sequence homology to the 5'UTR of *symE*, prevents initiation of translation by occluding the ribosome binding site and preventing ribosome loading. In this system, mRNA degradation is a secondary effect of the lack of translation and it does not require either Hfq or RNase III (26).

Most of the sRNAs identified thus far are unlinked to their target genes and, unlike *cis*-encoded sRNAs, their complementarity with their targets is only partial. Gene expression regulation mediated by *trans*-encoded sRNAs has been more extensively studied and the role of RNase E and Hfq has been well established (7,27,28) [review in

(29)]. One of the best characterized examples is the regulation of expression of several genes involved in iron metabolism by the RyhB sRNA. Masse *et al.* (6) showed that several target mRNAs are quickly degraded by RNase E upon RyhB binding. The rapid degradation of the target mRNAs required Hfq binding to the C-terminal scaffold region of RNase E (30). RyhB is codegraded upon binding the target mRNAs in an Hfq and RNase E scaffold-dependent manner (6). In the absence of Hfq, the half-life of RyhB was significantly reduced while in an Hfq RNase E double mutant, it was comparable to wild-type control, suggesting that Hfq stabilized RyhB by inhibiting RNase E mediated decay. Masse *et al.* (6) also showed that RNase III did not play a role in the RyhB-mediated degradation of its target *sodB*. A similar RNase E and Hfq-dependent mechanism has been described for the negative regulation of *ptsG* by the *trans*-encoded sRNA SgrS (8,9), suggesting a common mechanism of regulation by *trans*-encoded sRNAs. It has been speculated that pairing of *cis*-encoded sRNAs with extensive complementary to their target would not require the involvement of Hfq (10).

In this work, we wanted to characterize the role of ribonucleases and Hfq in the biogenesis and decay of the *cis*-encoded sRNA SibC, a Type I antitoxin responsible for the regulation the expression of the toxin IbsC. SibC is one of the five Sib (short, intergenic, abundant sequences) homologues found in the *E.coli* genome. The Sib sRNAs are the only antitoxin sRNAs known to date that have complete complementarity to the coding sequence of their targets (11). IbsC overexpression leads to the destabilization of the cell membrane, while SibC sRNA negatively regulates *ibsC* transcript levels (11).

Previous work done by Fozo *et al.* (11) showed that all 5 *sib* genes are constitutively expressed, but that these sRNAs accumulate in early-stationary phase. Northern blot analysis revealed the existence of two Sib transcripts of approximately 140 and 110 nucleotides in length that share identical 5' termini, but differ at their 3' ends (11). The longer transcripts have complete complementarity to the *ibs* coding sequences, including the ribosome binding sites, while the 3' ends of the shorter transcripts stop at the Shine-Dalgarno sequence of *ibs*. Fozo *et al.* (11) speculated that shorter form of Sib was the product of cleavage of the Sib/*ibs* duplex upon base pairing. However, this hypothesis was never tested. To get a better understanding of the processing pathways of Sib sRNAs and the mechanism by which they regulate *ibs* expression, we analyzed the role of the major endoribonucleases and Hfq in the processing and degradation of SibC and *ibsC* in *E.coli*.

Here we demonstrate that the shorter SibC transcript is not the result of processing of the SibC/*ibsC* duplex, since the shorter form was observed even in the absence of *ibsC* expression. In addition, we show that the endoribonucleases RNase III, RNase E, and RNase P all play a role in the processing of SibC. Interestingly, RNase III seems to protect SibC from degradation by an unknown mechanism. This role for RNase III in sRNA-mediated regulation of gene expression has not been previously described. We also show that in the absence of Hfq, the SibC sRNA is quickly degraded by RNase E. Unlike what has been reported for *sodB* (6), the degradation of SibC was not dependent of the C-terminal scaffold region of RNase E. Furthermore, in an *hfq* deletion strain the *ibsC* mRNA showed increased stability. Taken together, these observations

suggest a novel role for RNase P, RNase III, and Hfq in the negative regulation of *ibsC* by the *cis*-encoded sRNA SibC.

MATERIALS AND METHODS

Bacterial strains and plasmids

Strains and plasmids used in this study are listed in Table 2.1. The construction of the *sibAB/ibsAB* and *sibC/ibsC* chromosomal deletions was a multi-step process. First, MG1693, SK2525, SK4455, and SK5665 were transduced with P1 lysate grown on SK3279 (Δ *sibAB*/ Δ :*kan*). Kan^R transductants were first tested for the presence of the *sibAB* deletion via PCR using primers *sibABdelF2* and *sibABdelR*. Subsequently, strains SK4146-SK4149 were made electrocompetent and transformed with the arabinose inducible Flp recombinase plasmid, pCP20 (Tc^R and Ap^R), in the presence of arabinose to excise the kanamycin cassette inserted in *sibAB/ibsAB*, as previously described (12,13), generating strains SK1644-SK1647. These strains were grown in the absence of ampicillin to cure pCP20. Once each kanamycin cassette had been excised and the Flp plasmid lost, strains SK4137-SK4139 and SK4165 were transduced with P1 lysate grown on the GSO136 (Δ *sibC*/ Δ *ibsC*:*kan*) (11), provided by the Storz laboratory, to make strains SK3281-SK3284. Kan^R transductants were tested for the *sibC/ibsC* deletions via PCR using primers *sibCdelF2* and *sibCdelR*. Primers are listed in Table 2.2.

Once the chromosomal *sibABC/ibsABC* loci were deleted, strains SK3281-SK3284 were made electrocompetent and transformed with either pMRK3 to make strains SK3285-SK3288, pMRK6 to make strains SK3319-SK3322, or both, pMRK3 and pMRK6 to make strains SK3315-SK3318. SK3281 was also transformed with pMRK7 to make strain SK1641. SK3319 was transformed with pMRK7 to make SK1642.

The strain SK1643 was constructed by displacing pSBK1 from SK3727 with pMRK9.

The *hfq* deletion mutants, SK1635-SK1639, were constructed by transduction with P1 lysate grown on SK10246 (Table 2.1). Cm^R transductants were tested for the *hfq* deletion by PCR using primers HFQ735 and HFQ1057.

Plasmid constructions

pMRK3 is a single copy plasmid that contains an 808 bp *SibC* PCR fragment starting approximately 500 nucleotides upstream of the *sibC* transcription start site and including the downstream stem-loop structure that is thought to act as a Rho-independent transcription terminator (11). The *rrnB* terminator was cloned immediately after the *SibC* gene, but in the opposite strand to prevent transcription of the cis-encoded *ibsC*. Primers used are listed in Table 2.2. To amplify *SibC* from genomic MG1693 DNA, primers *sibC_BamHI* and *Bnrr_sibC* were used. The first primer had an engineered *BamHI* restriction site and the second one had a region complementary to the 3' end of the *rrnB* terminator. The *rrnB* terminator was amplified from pBMK31 (Mohanty and Kushner, unpublished results) using *Bnrr_end2start* and *Bnrr_ClaI* primers. pBMK31 was constructed by placing the *rrnB* terminator into the *ClaI* and *HindIII* sites of pBMK26 (14). Both PCR products were then amplified with *sibC_BamHI* and *Bnrr_ClaI* primers, digested with *BamHI* and *ClaI* restriction enzymes and cloned into the *BamHI* and *ClaI* sites of pVMK94, a pWSK29 (15) derivative with the mini-F single copy origin of DNA replication from pBK22 (16).

A similar strategy was used to construct pMRK6, a low-copy, IPTG inducible plasmid. The first step was to clone *ibsC* without its own promoter into pBMK11 (17).

The *lac* promoter in pBMK11 was amplified with primers pBMK_BamHI and pBMKibsC_R, the latter of which has complementarity with the coding region of IbsC. IbsC was amplified from MG1693 genomic DNA using primers pMRKibsC_F and ibsC_HindIII. Both PCR products were used as template for a PCR reaction with primers pBMK_BamHI and ibsC_HindIII. The overlapping fragment was digested with *Bam*HI and *Hind*III and cloned into the *Bam*HI and *Hind*III sites of pBMK11. This intermediate plasmid was called pMRK5. To prevent expression of *sibC*, the *rrnB* terminator was cloned into the opposite strand. It was amplified from pBMK31 using primers Brnn_end2start and pMRK_Brnn_R. The last PCR step was to amplify the *lac* promoter and *ibsC* region of pMRK5 with pBMK_BamHI and Brnn_ibsC_R primers and annealing the PCR product with the *rrnB* PCR fragment by an additional overlapping PCR reaction using primers pBMK_BamHI and pMRK_Brnn_R. pMRK_Brnn_R contains a *Cla*I restriction site. The end product of the overlapping PCR was digested with *Bam*HI and *Cla*I and cloned into the *Bam*HI and *Cla*I sites of pBMK11 to make pMRK6.

The pMKR7 plasmid was constructed similarly to pMRK3. It has the same 5' as pMRK3 but only has the first 112 nucleotides of SibC followed by the *leuU* Rho-independent transcription terminator instead of the endogenous stem loop that is thought to act as a terminator. SibC was amplified from pMRK3 using primers sibC_BamHI and pMRK7-1_R. The *leuU* terminator was amplified from wild-type genomic DNA using primers pMRK7-2F and pMRK7-3_R. The *rrnB* terminator was cloned after the *leuU* terminator in the opposite strand to prevent *ibsC* expression. It was amplified from pBMK31 using pMRK7-4_F and pMRKBrrn_R primers. Both terminators were used as template for the overlapping PCR using primers pMRK7-2_F and pMRK_Brnn_R. The

last overlapping step was to join the SibC product with both terminators by using primers sibC_BamHI and pMRK_Brrn_R. The end product was digested with *Bam*HI and *Cla*I and cloned into the *Bam*HI and *Cla*I sites of pVMK94 to make pMRK7.

The *rne-374* containing plasmid, pMRK9, was constructed by inserting the *Eco*RI/*Sac*I region of pMOK16 (18) into the *Eco*RI/*Sac*I sites of streptomycin/spectinomycin resistant pMOK18 (19).

Growth conditions

One mL of a standing overnight culture grown at 30°C was used to inoculate 25 mL of Luria-Bertani broth. Strains harboring chromosomal mutations were grown on LB broth supplemented with 50 µg/ml of thymine. The medium used to grow strains containing plasmids was also supplemented with 20 µg/ml of chloramphenicol, 25 µg/ml of kanamycin, 20 µg/ml streptomycin, or 50 µg/ml of ampicillin, as necessary. Most of the experiments described here were conducted in early stationary phase. Strains harboring the temperature sensitive alleles (*rne-1* and *rnpA49*) were grown shaking at 30°C and switched to 44°C an hour before entering stationary phase. All other strains were grown shaking at 44°C into early stationary phase, at which point the samples were collected. A Klett-Summerson colorimeter with a green filter, no. 42, was used to measure growth.

For half-life experiments, 500 µg/ mL of rifampicin and 20 µg/ mL of nalidixic acid were added to the cultures as they entered early stationary phase and the first time points were collected 80 seconds after addition. Subsequent samples were collected at different time points as indicated in the figures.

Cell viability assays

For *ibsC* induction experiments, bacterial strains were grown into mid-exponential phase (Klett 150, as measured by a Klett-Summerson colorimeter with a green filter, no. 42). Cultures were then split in half and 250 μ M of IPTG was added to one flask. Samples were collected at different times as indicated in the figures.

RNA isolation

When cultures entered stationary phase, two mL aliquots were added to 8 mL of TM crushed-ice buffer with a final concentration of 10mM Tris pH 7.2, 5mM magnesium chloride, 20 mM sodium azide, 0.4mg/ml chloramphenicol and spun at 3100xg for 10 minutes. Cell pellets were immediately frozen in a dry-ice ethanol bath and stored at -80°C. Pellets were then thawed at 37°C for 8 seconds and resuspended in 1 mL of Trizol[®] (Invitrogen), vortexed for 30 seconds, placed on ice for 30 seconds, and vortexed for another 30 seconds. Samples were then incubated at room temperature for 5 min before adding 200 μ L of chloroform, shaking vigorously for 45 seconds, and incubating at room temperature for 3 minutes. Samples were then spun down at 12000xg for 15 min and 600 μ L of the aqueous phase were transferred to a new microfuge tube with 900 μ L of isopropanol and incubated at 4°C overnight. RNA was pelleted at 12000xg for 10 minutes, washed with 75% ethanol and spun at 7500xg for 5 min. Ethanol was aspirated and the pellet was air-dried for approximately 12 minutes. RNA was resuspended in RNase-free water and quantified using a Nanodrop 2000c (Thermo Scientific).

Northern Blotting

Ten μ g of total RNA were mixed with an equal volume of Gel loading Buffer II (Ambion) and resolved on 8%/8.3M urea polyacrylamide denaturing gels in 1X TBE.

RNA was transferred to Nytran SPC membranes (Whatman) at 50V for one hour at 4°C. Membranes were subsequently baked at 80°C for 30 minutes and UV cross-linked for 20 seconds. Before probing, membranes were washed in 2% SSC and incubated in PerfectHyb buffer (Sigma) at 50°C. T4 polynucleotide kinase (New England Biolabs) was used according to manufacturer's recommendations to end label the probes listed in Table 2.2. Membranes were hybridized overnight at 50°C, washed four times in 2X SSC/0.1% SDS, twice at room temperature and twice at 50°C. Membranes were exposed to phosphor screens and the screens were scanned using a Storm 840 Phosphorimager (GE Healthcare). Band intensities were determined using ImageQuant 5.2 software (GE Healthcare).

RESULTS

Processing of the primary SibC transcript at 44°C involves RNase E, RNase P and RNase III.

It has previously been reported that in early stationary phase cells of *E. coli* there are two forms of the SibC sRNA, a presumed full-length species (141 nt) (Fig. 2.1A) and a shorter processed form of 109 nt (11). In order to determine which endonuclease was responsible for generating the shorter form, we initially examined an isogenic series of strains carrying mutations in RNase E, RNase P and RNase III by Northern blot analysis of steady-state RNAs isolated from the strains grown at 30°C. We observed a slight increase (2-4 fold) in the steady-state level of SibC141, the longer form of SibC, in all three *rne-1* strains (*rne-1*, *rne-1 rnc-14*, and *rne-1 rnpA49*) as compared to wild-type control (Figure 2.2, lanes 1, 4, 5, and 7). Interestingly, there were no changes observed in the smaller form of SibC, SibC109 in any of the strains tested (Fig. 2.2, lanes 1-7).

Since the *rne-1* and the *rnpA49* alleles encode temperature sensitive RNase E and RNase P proteins, respectively, we repeated the experiment at 44°C to determine if inactivation of either endonuclease altered the biogenesis of the SibC109 species. To our surprise, we observed an additional smaller species of 111 nt at 44°C, SibC111 (Fig. 2.2, lane 8). Based on the data obtained from the *rnpA49* and *rne-1* single mutants, RNase E is involved in the generation of SibC109 and RNase P is required for SibC111 (Fig. 2.2, lanes 9 and 11). Unexpectedly, in the absence of RNase III, there was a dramatic reduction in the levels of both smaller species (Fig. 2.2, lane 10). Furthermore there was no detectable smaller species in the *rnc-14 rne-1* double mutant (Fig. 2.2, lane 14).

At non-permissive temperature, the total amount of SibC RNAs was higher than at 30°C. In addition, similar to what we observed at 30°C, the steady-state levels of SibC141 were higher in the *rne-1* strains than in wild-type (Figure 2.2, lanes 8, 11, 12, and 14). The levels of SibC141 were also higher in the *rnpA49* strain than in the wild-type control, but not as high as *rne-1* (Figure 2.2, lanes 8 and 9). Interestingly, only in the *rnc-14* strain was the steady-state level of SibC lower than in the wild-type control (Figure 2.2, lanes 8 and 10). In the *rne-1 rnc-14* double mutant, we detected more SibC RNA than in wild-type and *rnc-14* strains, but less than in the *rne-1* single mutant.

In the *rnpA49* strain the level of SibC111 was highly reduced as compared to the wild-type control, but SibC109 levels were higher. (Figure 2.2, lane 9). This result suggested that RNase P was required for the production of SibC111. In the *rnc-14* and the *rnc-14 rnpA49* double mutant strains, SibC111 was barely visible (Figure 2.1, lanes 10 and 13). These results indicated that RNase III activity was involved prior to RNase P in order to generate SibC111. Since our data suggested that RNase E was required for

the production of SibC109 and RNase III activity was required for RNase P to generate SibC111, it was not surprising that in the *rne-1 rnc-14* double mutant, both species were largely absent (Figure 2.1, lane 14). In agreement with this, in the absence of RNase III and RNase P, SibC109 was still generated by RNase E (Figure 2.1, lane 13).

To determine if the SibC processing observed in wild-type cells required the formation of a SibC/*ibsC* duplex, we examined SibC in cells that only expressed the sRNA, but not its target *ibsC* mRNA. Since it has been reported that *ibsA* might interact with more than one Sib sRNA (11), the *sibAB/ibsAB* and the *sibC/ibsC* loci were all deleted from the chromosome and the triple deletion mutant was transformed with pMRK3 (Figure 2.1B), a single-copy vector expressing *sibC* from its endogenous promoter without expressing *ibsC* from the opposite strand. As expected, in a strain lacking all three *sibABC/ibsABC* loci, when SibC was expressed from pMRK3 (Table 2.1) at 44°C, the same three species as seen in Fig. 2.2, lane 8 were observed (Fig. 2.3, lanes 1 and 2). The lack of *ibsC* expression from pMRK3 was confirmed via Northern analysis (Figure 2.3B). Fozo *et al.* (11) have previously reported that *ibsC* was only visible if the *sibC* promoter was deleted or in the absence of RNase III activity. None of the strains containing the pMRK3 plasmid expressed full-length *ibsC*, including the *rnc-14 ΔsibABC/ibsABC* multiple mutant (Figure 2.3, panel B, lane 8).

Overall, at 44°C the results obtained when SibC was expressed in the absence of its target *ibsC* mRNA were identical to those obtained in the presence of coupled expression (Figure 2.3).

Endoribonucleases control the levels of SibC in the cell

The changes in the steady-state levels of SibC that were observed in the different ribonuclease mutants could have arisen from either altered levels of transcription or changes in the stability of the SibC sRNA. To address this question, we determined the chemical half-life of SibC141 species in the various ribonuclease mutants at 44°C. These experiments were carried out as described in the Materials and Methods. In the wild-type control, SibC141 had a half-life of 9.0 min, while it decreased to 7.2 min in *rnc-14* single mutant, but increased to 12.6 min in an *rne-1* strain (Figure 2.4, panels A,C, and E). These results suggested that the decrease in the steady-state levels of SibC141 observed in the *rnc-14* mutant and the increase observed in the *rne-1* strain as compared to wild-type control were due to changes in the stability of the sRNA and not changes in transcription. The increase in the stability SibC141 in an *rne-1* mutant suggested that RNase E plays a role in the decay/processing of SibC141. The decrease in the half-life of SibC141 in the absence of RNase III, fits well with the reduced steady-state levels that were observed in Figs. 2.2 and 2.3. In fact, these data suggest that RNase III may be directly or indirectly protecting SibC from cleavage. Interestingly, in an RNase III, RNase E double mutant the half-life of SibC141 was 8.4 min, comparable to what we observed in the wild-type control, but not as stable as what was observed in the *rne-1* single mutant (Table 2.3). This result suggests that RNase III is not protecting SibC from RNase E activity.

In the case of RNase P, the steady-state levels of SibC increased at 44°C compared to the wild-type control (Figure 2.2, lanes 8 and 9). However, the half-life of SibC141 in *rnpA49* decreased from 9.0 min in wild-type to 6.3 min (Figure 2.4, panels A

and G). This result suggested that the increase in steady-state level observed in *rnpA49* was not due to increased stability of SibC. Alternatively, the change in steady-state level might be the result of increased transcription.

Next, we wanted to determine if the changes in the stability of SibC in the different ribonuclease mutants were related to the processing/decay of the SibC/*ibsC* duplex. For this experiment, we measured the decay of SibC in strains where only the sRNA was expressed. Interestingly, in the absence of *ibsC* target, the half-life of SibC141 was shorter than when the target was present, 7.0 min versus 9.0 min, respectively (Figure 2.4, panels A and B). However, we did not observe any differences in the half-life of SibC141 in the presence or absence of *ibsC* in *rnc-14* and *rnpA49* mutants, suggesting that RNase III and RNase P activity was independent of target mRNA (Figure 2.4, panels B,C,D, and E). It is possible that both of these enzymes participate in the degradation of unbound SibC. In the case of RNase E mutants, the half-life of SibC141 increased significantly in the absence of target (Figure 2.4, panels E and F). This finding suggested a major role for RNase E in the decay of free SibC, as well as in the decay of the SibC/*ibsC* duplex.

The role of Hfq in the regulation of the *cis*-encoded sRNA SibC

SibC has been shown to co-immunoprecipitate with the RNA chaperone Hfq (20). However, according to Fozo *et al.* (11), Hfq did not change the steady-state levels of the SibC and *ibsC* RNAs in the cell. To confirm these findings, we determined the half-life of SibC in a Hfq deficient strain. Surprisingly, in the absence of Hfq the half-life of SibC was significantly shorter (5.5 min) compared to 9.0 min in the wild-type control (Figure 2.5, panel B and Table 2.4). The Hfq effect on the stability of SibC was independent of

SibC/*ibsC* duplex formation, since the half-life of SibC in the Hfq mutant strain expressing only the sRNA was comparable (6.4 min) to that of the Hfq mutant expressing both, the target and the sRNA (Figure 2.5, panels B, E, and Table 2.4).

To determine if Hfq possibly protects SibC from RNase E-dependent degradation, we examined the stability of SibC in an *hfq-10 rne-1* double mutant. In the absence of both, RNase E and Hfq, SibC141 had a half-life of 25.4 min (Figure 2.5, panel C and Table 2.4), a dramatic increase from what was observed in either single mutant (Table 2.4). What was also interesting about this result was that even though SibC141 had a significantly shorter half-life in the *hfq-10* single mutant, in the double mutant the half-life increased dramatically. This result suggested that RNase E is necessary for the rapid degradation of SibC in absence of Hfq. The observed increase in stability was target-independent, strengthening the hypothesis that Hfq binds unbound SibC and protects it from RNase E-dependent degradation (Figure 2.5, panel F and Table 2.4).

The RNase E-based degradosome plays a role in the biogenesis and decay of the SibC141 sRNA

Morita *et al.* (21) reported that Hfq binds the scaffold region of RNase E. Therefore, we wanted to determine if the synergistic effect on SibC stability observed in the *rne-1 hfq* double mutant on was mediated via the scaffold region of the RNase E-based degradosome. To test this hypothesis, we took advantage of the *rneΔ374* deletion, which lacks the entire scaffold region of RNase E but exhibits mRNA half-lives almost identical to the wild-type control (18). In fact, in the *rneΔ374* genetic background the half-life of SibC141 was 4.6 min, considerably shorter than in the wild-type control and comparable to what we observed in the Hfq deletion strain (Figure 2.5, panels B, D and

Table 2.4). The decrease in stability observed in the *rneΔ374* strain suggested that the protective effect Hfq has on SibC is mediated by the scaffold region of RNase E. Furthermore, when the Hfq deletion was combined with the *rneΔ374* allele, the SibC had a half-life (3.4 min), was comparable to what was observed in either single mutant.

We also examined if Hfq had an effect on RNase III-mediated decay of SibC by looking at an *rnc-14 hfq* double mutant. The combination of alleles had an additive effect on the half-life of SibC141. As previously shown, the half-life of SibC141 decreased from 9 min in a wild-type control to 7.2 min in the absence of RNase III (Table 2.3). In an *rnc-14 hfq* double mutant, SibC became more unstable, with a half-life of 3.8 min (Table 2.4). This half-life was shorter than what we observed in the *rnc-14* and *hfq* single mutants. Taken together, these results suggested that both RNase III and Hfq protect SibC from RNase E activity. Interestingly, in the absence of *ibsC* expression, the half-life of SibC141 in the *hfq rne-1* double mutant was 9.6 min. This value was comparable to what we obtained in the wild-type control strain (Table 2.3), which further supports the hypothesis that the rapid decay of SibC in the absence of RNase III and Hfq is target dependent.

Are the shorter forms of SibC involved in *ibsC* regulation

Fozo *et al.* (11) showed that the shorter SibC transcript lacks approximately 30 nucleotides at the 3' end of full-length SibC RNA. They hypothesized that the shorter form was likely the result of processing of the SibC-*ibsC* RNA duplex. However, we have shown here that this is not the case since the shorter forms of SibC were observed in cells in which *ibsC* was not expressed (Figure 2.3). Therefore, if the shorter form(s) of

SibC do not result from the target-coupled decay of SibC, it is possible that the shorter form(s) have biological activity.

In order to determine if the shorter form of SibC was capable of target regulation, we constructed pMRK7, a plasmid similar to pMRK3, but expressing only the first 111 nucleotides form of SibC, followed by the *leuU* Rho-independent terminator (22) (Figure 2.1D). pMRK7 was then transformed into strains lacking the chromosomal *sibAB/ibsAB* and *sibC/ibsC* loci. These cells were also transformed with pMRK6, an IPTG-inducible plasmid expressing *ibsC* (Figure 2.1C). The presence of only SibC111 in the cell was confirmed by Northern analysis (Figure 2.6, panel B, lane 17).

To ascertain if the short form of SibC was functional, we examined its ability to counteract the toxicity of *ibsC* overexpression. For these experiments, we determined the percentage of viable cells 10 minutes after *ibsC* induction by comparing cell counts in induced versus uninduced cultures. When both forms of SibC were expressed (pMRK3), 1.7 ± 0.4 % of the cells survived the 10 min induction, while 2.5 ± 0.1 % of the population survived when only the short form of SibC (pMRK7) was expressed (data not shown). These results suggested that the shorter form of SibC was able to regulate the expression of *ibsC*. However, when we examined survival after *ibsC* induction in cells without SibC expression, we observed a 6.7 ± 1.6 % of survival (data not shown). The higher survival in cells expressing the toxin but not antitoxin was completely unexpected.

To further investigate how the different forms of SibC might differ in their capacity to regulate *ibsC* expression, we analyzed the decay of *ibsC* transcript in cells expressing SibC from either pMRK3 (both forms) or pMRK7 (short form). In order to determine the half-life of *ibsC*, we induced *ibsC* expression by adding 250 μ M of IPTG

to the cultures and inhibited new transcription by adding rifampicin 5 minutes after induction. Our analysis revealed no differences in the processing of *ibsC* between the two strains, the band pattern and the decay rate were the same (Figure 2.6). Interestingly, no difference was observed when *ibsC* was induced in the absence of SibC (Figure 2.8). These results could be due to a saturation of the system. The high levels of *ibsC* after induction could lead to the quick degradation of the pool of available SibC in cell. Even though new SibC transcription was taking place, it might not be strong or fast enough to allow us to observe any differences in the presence or absence of the sRNA.

Surprisingly, we observed a larger SibC band after *ibsC* induction (~160 nucleotides). This larger band disappeared as *ibsC* levels increased and was not present under normal levels of *ibsC* expression (Figure 2.7, panel A). A bigger SibC transcript (~130 nucleotides) was also observed when only the shorter form of SibC was expressed (pMRK7) (Figure 2.6, panel B, lane 18 and Figure 2.7, panel A). The origin of these new transcripts is not known at this time. When a probe complementary to the 5' upstream of the -10 and -35 region of *sibC* was used, we did not observe any bands (data not shown). We also tested a probe designed against the *leuU* terminator that was used to stop transcription in the pMRK7 plasmid (Figure 2.3, panel D). This probe failed to produce the ~130 nucleotide band. These results seemed to eliminate the possibility of a bigger transcript due to the use of an alternative promoter. The SibC130 band observed does not seem to arise from read-through past the *leuU* terminator. It should be noted that a faint, slightly larger SibC transcript has also been observed in *rnc-14* mutant strains (Figure S.2.1). Further experiments are needed to determine the origin of these new transcripts and their relevance in regulating the expression of *ibsC*.

Upon *ibsC* induction, we observed a smear of bands bigger than the 160 nucleotide full-length *ibsC* transcript observed in RNase III mutants (Figure 2.6, panel A; Figure 2.7, panel B; Figure 2.8). Bigger transcripts have also been observed in strains expressing *ibsC* from the chromosome (data not shown). To determine if these transcripts were due to read-through past the stem loop structure predicted to cause transcription termination (23), we designed a probe against the *rrnB* terminator that was cloned on the opposite strand (Figure 2.3 C). The two biggest bands annealed to the probe (data not shown), which would suggest that the predicted terminator was weak and read-through past it likely occurs. After induction, these read-through transcripts were efficiently processed into a single, 160 nucleotide band in the ribonuclease wild-type strain (Figure 2.8, lanes 1-8). In the *rne-1* mutant, these read-through transcripts were still present 15 minutes after new transcription was inhibited by rifampicin and there was very little full-length (160 nucleotide) *ibsC* (Figure 2.8, lanes 9-14). These results suggest that RNase E efficiently processes the 3' end of the *ibsC* transcript.

DISCUSSION

Although great progress has been made in the identification of bacterial toxin-antitoxin systems as well as the discovery of small, regulatory RNAs, their characterization is still at an early stage. In this work, we have shown that RNase III, RNase E, and RNase P, all play a role in the biogenesis and decay of the *cis*-encoded sRNA SibC. Our work demonstrates that the metabolism of SibC, as well as the SibC-mediated regulation of *ibsC* expression is much more complicated than previously thought. Surprisingly, the RNA chaperone Hfq also plays a role in the stability of SibC and *ibsC* mRNA.

Our data have shown that the processing of the full-length SibC transcript (SibC141) into the smaller SibC111 and SibC109 species is mediated by multiple endoribonucleases (Figure 2). Inactivation of RNase P at 44°C resulted in a reduction in the steady-state level of SibC111. The steady-state level of SibC111 was also lower in an RNase III deletion strain. In contrast, RNase E inactivation led to a decrease in the steady-state level of SibC109. Taken together these results suggested that RNase III activity was needed for the RNase P-mediated generation of SibC111 and RNase E activity was required for the generation of SibC109.

The interaction of these ribonucleases in the processing mechanism of SibC141 was further supported by the analysis of a combination of double mutants. In the absence of RNase III and RNase P, SibC109 was still generated by RNase E, while in the absence of RNase E and RNase III there were no detectable smaller species. Interestingly, contrary to what has been previously speculated (11), we showed that none of these processing events were the result of SibC/*ibsC* duplex processing, since there were no significant differences in processing between strains expressing SibC and *ibsC* and strains expressing only SibC (Figure 2.3).

Our work here has also demonstrated that the SibC/*ibsC* system shares features of both *cis*- and *trans*-encoded sRNA-mediated regulation of gene expression. We have shown that RNase III had a protective effect on the SibC RNA, while it negatively regulates *ibsC* expression. As shown in Figure 2.4, the observed decrease in the stability of SibC141 was likely the result of increased processing by ribonucleases, since the half-life of SibC141 decreased from what was observed in the wild-type control. Furthermore,

we showed that in the absence of RNase III and RNase E activity, the half-life of SibC141 was comparable to the wild-type control, but not as stable as what was observed in the *rne-1* single mutant. These results suggest that RNase III may stabilize SibC independent of RNase E activity. It is possible that RNase III is indirectly affecting the stability of SibC by regulating the levels of other ribonucleases.

We also confirmed the results previously reported by *Fozo et al.* (11) on the effect of RNase III in the stability of the *ibsC* mRNA. As shown in Figure 2.2, in the absence of RNase III, the *ibsC* mRNA was stabilized sufficiently so that it could be seen in a Northern blot.

Furthermore, we have demonstrated a role for Hfq and RNase E in the metabolism of SibC similar to what has been reported for RyhB (6). Figure 2.2 shows that upon the inactivation of RNase E at 44°C, the steady-state levels of SibC increased. Furthermore, the half-life of SibC141 was longer in an *rne-1* mutant than what we observed in the wild-type control (Figure 2.4). We also have shown that Hfq protects SibC141 from RNase E-mediated degradation similar to what was described for the *trans*-encoded sRNA RyhB, since in the absence of Hfq the half-life of SibC141 decreased and in the *hfq rne-1* double mutant it became significantly longer, even more so than the *rne-1* single mutant (Figure 2.5). Interestingly, we also showed that although the protection of SibC mediated by Hfq was dependent on RNase-E based degradosome, the RNase E-mediated degradation of SibC was not dependent on the the C-terminal region of RNase E (Figure 2.5). The half-life of SibC141 was comparable between the Hfq mutant and the *rneΔ374* deletion strain.

In addition to the Hfq interaction with the C-terminal domain of RNase E (21,31), several other proteins are known to bind to the scaffold region of RNase E to form a multi-protein complex known as the degradosome. Among these proteins are the RNA helicase RhlB, the glycolytic enzyme enolase, and the 3' to 5' exonuclease polynucleotide phosphorylase (PNPase) [reviewed in (32)]. Surprisingly, enolase has been shown to play a role in sRNA-mediated regulation of gene expression. The rapid degradation of *ptsG* mRNA upon SgrS binding requires the presence of enolase in the RNaseE-based degradosome (9).

PNPase has also been shown to play a role in sRNA degradation in the absence of Hfq (33). It would be interesting to determine if PNPase is also involved in the metabolism of SibC via its interaction with RNase E (34), its interaction with Hfq (35), or by itself. For example, it is possible that the significant increase in the half-life of SibC observed in the *rne-1 hfq* double mutant could be the result of failure to recruit PNPase to the sRNA by either RNase E or Hfq.

To our knowledge, the *SibC/ibsC* system is one of only two systems characterized thus far in which Hfq has been shown to play a role in *cis*-encoded sRNA-mediated regulation. While this manuscript was in preparation, Ross *et al.* (36) published their findings on Hfq binding to RNA-IN and RNA-OUT and facilitating their interaction in the *Tn10-IS10* system. Further characterization of additional *cis*-encoded sRNAs and their mechanisms for regulating gene expression may reveal a more prevalent role of Hfq in their regulation than previously thought.

It should be noted that a possible caveat of the approach we have taken here was the use of rifampicin to determine the half-life of SibC. When analyzing sRNA metabolism by treating the cells with rifampicin to inhibit global transcription initiation, there is always the concern of destabilizing the sRNA by depleting it of its target mRNA. However, the steady-state level of SibC was not significantly different in the absence of *ibsC* than when both SibC and *ibsC* were expressed (Figure 2.3). Furthermore, if the sRNA became destabilized due to the depletion of the target mRNA by the addition of rifampicin, we would expect to see no differences in the half-life of the sRNA between a wild-type strain and a strain where the target had been deleted because eliminating the target pool with rifampicin would be equivalent to the target deletion. Since, we did observe differences in the half-life of SibC when comparing strains expressing SibC by itself and strains expressing the sRNA and the target we were not concerned that this was case (Figure 2.4). It would still be interesting to compare the results presented here to half-lives determined by expressing SibC from an inducible plasmid and measuring the decay after the inducer was removed. It would allow us to confirm that what we observed in these experiments was not the effect of using rifampicin.

The combination of the inducible *ibsC* plasmid (pMRK6) with an inducible SibC plasmid could also help us determine if all forms of SibC are functionally active. Our attempt to do so by increasing the levels of *ibsC* expression while SibC was endogenously expressed did not allow us to address the question of the functional nature of the shorter forms of SibC. This set-back could be due to a saturation of the system. A five minutes induction of *ibsC* expression could potentially lead to the rapid degradation of SibC in the cell in an attempt to prevent the toxicity of *ibsC* overexpression. Therefore,

the lack of differences observed after *ibsC* induction by itself or in conjunction with SibC expression from the pMRK3 and pMRK7 plasmids could simply reflect *ibsC* processing after the pool of SibC RNA had been depleted. A plasmid with inducible SibC expression would allow us to fine-tune the levels of both RNAs and therefore, to analyze *ibsC* processing when SibC is in excess. These studies would help us better understand the SibC-mediated events involved in the regulation of expression of *ibsC*.

ACKNOWLEDGEMENTS

This work was supported in part by a grant from the National Institute of General Medical Sciences to S.R.K.

REFERENCES

1. Wagner, E.G. and Simons, R.W. (1994) Antisense RNA control in bacteria, phages, and plasmids. *Annu. Rev. Microbiol.*, 48, 713-742.
2. Storz, G., Opdyke, J.A. and Zhang, A. (2004) Controlling mRNA stability and translation with small, noncoding RNAs. *Curr. Opin. Microbiol.*, 7, 140-144.
3. Mizuno, T., Chou, M.Y. and Inouye, M. (1984) A unique mechanism regulating gene expression: translational inhibition by a complementary RNA transcript (micRNA). *Proc. Natl. Acad. Sci. U S A*, 81, 1966-1970.
4. Gerdes, K., Rasmussen, P.B. and Molin, S. (1986) Unique type of plasmid maintenance function: postsegregational killing of plasmid-free cells. *Proc. Natl. Acad. Sci. U S A*, 83, 3116-3120.
5. Gerdes, K., Nielsen, A., Thorsted, P. and Wagner, E.G. (1992) Mechanism of killer gene activation. Antisense RNA-dependent RNase III cleavage ensures

- rapid turn-over of the stable *hok*, *srnB* and *pndA* effector messenger RNAs. *J. Mol. Biol.*, 226, 637-649.
6. Masse, R., Escorcia, F.E. and Gottesman, S. (2003) Coupled degradation of a small regulatory RNA and its mRNA targets in *Escherichia coli*. *Genes Dev.*, 17, 2374-2383.
 7. Moller, T., Franch, T., Hojrup, P., Keene, D.R., Bachinger, H.P., Brennan, R.G. and Valentin-Hansen, P. (2002) Hfq: a bacterial Sm-like protein that mediates RNA-RNA interaction. *Mol. Cell*, 9, 23-30.
 8. Kimata, K., Tanaka, Y., Inada, T. and Aiba, H. (2001) Expression of the glucose transporter gene, *ptsG*, is regulated at the mRNA degradation step in response to glycolytic flux in *Escherichia coli*. *EMBO J.*, 20, 3587-3595.
 9. Morita, T., Kawamoto, H., Mizota, T., Inada, T. and Aiba, H. (2004) Enolase in the RNA degradosome plays a crucial role in the rapid decay of glucose transporter mRNA in the response to phosphosugar stress in *Escherichia coli*. *Mol. Microbiol.*, 54, 1063-1075.
 10. Waters, L.S. and Storz, G. (2009) Regulatory RNAs in bacteria. *Cell*, 136, 615-628.
 11. Fozo, E.M., Kawano, M., Fontaine, F., Kaya, Y., Mendieta, K.S., Jones, K.L., Ocampo, A., Rudd, K.E. and Storz, G. (2008) Repression of small toxic protein synthesis by the Sib and OhsC small RNAs. *Mol. Microbiol.*, 70, 1076-1093.
 12. Baba, T., Ara, T., Hasegawa, M., Takai, Y., Okumura, Y., Baba, M., Datsenko, K.A., Tomita, M., Wanner, B.L. and Mori, H. (2006) Construction of *Escherichia*

- coli* K-12 in-frame, single-gene knockout mutants: the Keio collection. *Mol. Sys. Biol.*, 2, 2006 0008.
13. Cherepanov, P.P. and Wackernagel, W. (1995) Gene disruption in *Escherichia coli*: TcR and KmR cassettes with the option of Flp-catalyzed excision of the antibiotic-resistance determinant. *Gene*, 158, 9-14.
 14. Perwez, T. and Kushner, S.R. (2006) RNase Z in *Escherichia coli* plays a significant role in mRNA decay. *Mol. Microbiol.*, 60, 723-737.
 15. Wang, R.F. and Kushner, S.R. (1991) Construction of versatile low-copy-number vectors for cloning, sequencing and expression in *Escherichia coli*. *Gene*, 100, 195-199.
 16. Babitzke, P. and Kushner, S.R. (1991) The Ams (altered mRNA stability) protein and ribonuclease E are encoded by the same structural gene of *Escherichia coli*. *Proc. Natl. Acad. Sci. U S A*, 88, 1-5.
 17. Mohanty, B.K. and Kushner, S.R. (1999) Analysis of the function of *Escherichia coli* poly(A) polymerase I in RNA metabolism. *Mol. Microbiol.*, 34, 1094-1108.
 18. Ow, M.C., Liu, Q. and Kushner, S.R. (2000) Analysis of mRNA decay and rRNA processing in *Escherichia coli* in the absence of RNase E-based degradosome assembly. *Mol. Microbiol.*, 38, 854-866.
 19. Ow, M.C. and Kushner, S.R. (2002) Initiation of tRNA maturation by RNase E is essential for cell viability in *Escherichia coli*. *Genes Dev.*, 16, 1102-1115.
 20. Zhang, A., Wassarman, K.M., Rosenow, C., Tjaden, B.C., Storz, G. and Gottesman, S. (2003) Global analysis of small RNA and mRNA targets of Hfq. *Mol. Microbiol.*, 50, 1111-1124.

21. Morita, T., Maki, K. and Aiba, H. (2005) RNase E-based ribonucleoprotein complexes: mechanical basis of mRNA destabilization mediated by bacterial noncoding RNAs. *Genes Dev.*, 19, 2276-2186.
22. Mohanty, B.K. and Kushner, S.R. (2008) Rho-independent transcription terminators inhibit RNase P processing of the *secG leuU* and *metT* tRNA polycistronic transcripts in *Escherichia coli*. *Nucleic Acids Res.*, 36, 364-375.
23. Han, K., Kim, K.S., Bak, G., Park, H. and Lee, Y. (2010) Recognition and discrimination of target mRNAs by Sib RNAs, a cis-encoded sRNA family. *Nucleic Acids Res.*, 38, 5851-5866.
24. Opdyke, J.A., Fozo, E.M., Hemm, M.R. and Storz, G. (2011) RNase III participates in GadY-dependent cleavage of the *gadX-gadW* mRNA. *J. Mol. Biol.*, 406, 29-43.
25. Takada, A., Umitsuki, G., Nagai, K. and Wachi, M. (2007) RNase E is required for induction of the glutamate-dependent acid resistance system in *Escherichia coli*. *Biosci., Biotech., Biochem.*, 71, 158-164.
26. Kawano, M., Aravind, L. and Storz, G. (2007) An antisense RNA controls synthesis of an SOS-induced toxin evolved from an antitoxin. *Mol. Microbiol.*, 64, 738-754.
27. Zhang, A., Wassarman, K.M., Ortega, J., Steven, A.C. and Storz, G. (2002) The Sm-like Hfq protein increases OxyS interaction with target mRNAs. *Mol. Cell*, 9, 11-22.
28. Vogel, J. and Luisi, B.F. (2011) Hfq and its constellation of RNA. *Nat. Rev.*, 9, 578-589.

29. Gottesman, S. (2004) The small RNA regulators of *Escherichia coli*: Roles and mechanisms. *Annu. Rev. Microbiol.*, 58, 303-328.
30. Ikeda, Y., Yagi, M., Morita, T. and Aiba, H. (2011) Hfq binding at RhlB-recognition region of RNase E is crucial for the rapid degradation of target mRNAs mediated by sRNAs in *Escherichia coli*. *Mol. Microbiol.*, 79, 419-432.
31. Aiba, H. (2007) Mechanism of RNA silencing by Hfq-binding small RNAs. *Curr. Opin. Microbiol.*, 10, 134-139.
32. Carpousis, A.J. (2002) The *Escherichia coli* degradosome: Structure, function and relationship to other ribonucleolytic multienzyme complexes. *Biochem. Soc. Trans.*, 30, 150-155.
33. Andrade, J.M., Pobre, V., Matos, A.M. and Arraiano, C.M. (2012) The crucial role of PNPase in the degradation of small RNAs that are not associated with Hfq. *RNA*, 18, 844-855.
34. Vanzo, N.F., Li, Y.S., Py, B., Blum, E., Higgins, C.F., Raynal, L.C., Krisch, H.M. and Carpousis, A.J. (1998) Ribonuclease E organizes the protein interactions in the *Escherichia coli* RNA degradosome. *Genes Dev.*, 12, 2770-2781.
35. Mohanty, B.K., Maples, V.F. and Kushner, S.R. (2004) The Sm-like protein Hfq regulates polyadenylation dependent mRNA decay in *Escherichia coli*. *Mol. Microbiol.*, 54, 905-920.
36. Ross, J.A., Ellis, M.J., Hossain, S. and Haniford, D.B. (2013) Hfq restructures RNA-IN and RNA-OUT and facilitates antisense pairing in the Tn10/IS10 system. *RNA*, (in press).

37. Stead, M.B., Marshburn, S., Mohanty, B.K., Mitra, J., Pena Castillo, L., Ray, D., van Bakel, H., Hughes, T.R. and Kushner, S.R. (2011) Analysis of *Escherichia coli* RNase E and RNase III activity in vivo using tiling microarrays. *Nucleic Acids Res.*, 39, 3188-3203.
38. Arraiano, C.M., Yancey, S.D. and Kushner, S.R. (1988) Stabilization of discrete mRNA breakdown products in *ams pnp rnb* multiple mutants of *Escherichia coli* K-12. *J. Bacteriol.*, 170, 4625-4633.

Table 2.1. Bacterial strains and plasmids used in this study.

Strain	Genotype	Source of reference
GSO136	MG1655 Δ sibC/ Δ ibsC:: <kan< td=""> <td>(11)</td> </kan<>	(11)
MG1693	<i>thyA715 rph-1</i>	<i>E.coli</i> Genetic Stock Center
SK1635	SK5665 (<i>rne-1</i>) <i>hfq-10</i>	This study
SK1636	SK3288 [(Δ sibABC/ Δ ibsABC <i>rne-1</i>)/ pMRK3 (SibC)] <i>hfq-10</i>	This study
SK1637	SK3285 [(Δ sibABC/ Δ ibsABC)/ pMRK3 (SibC)] <i>hfq-10</i>	This study
SK1638	SK4455 (<i>rnc-14</i>) <i>hfq-10</i>	This study
SK1639	SK3287 [(Δ sibABC/ Δ ibsABC <i>rnc-14</i>)/ pMRK3 (SibC)] <i>hfq-10</i>	This study
SK1641	SK3281 (Δ sibABC/ Δ ibsABC)/ pMRK7 (SibC111)	This study
SK1642	SK3319 [(Δ sibABC/ Δ ibsABC)/ pMRK6 (ibsC)]/ pMRK7 (SibC111)	This study
SK1643	<i>rne</i> Δ 1018:: <bla <i="">thyA715 rph-1 hfq-1::Ω/ pMRK9 (<i>rne</i>Δ374)</bla>	This study
SK1644	SK4146 /pCP20	This study
SK1645	SK4147/ pCP20	This study
SK1646	SK4148/ pCP20	This study
SK1647	SK4149/ pCP20	This study
SK2525	<i>rnpA49 thyA715 rph-1 rbsD296</i> ::Tn10 Tc ^R	(19)
SK3279	MG1655 Δ sibAB/ Δ ibsAB ::kan	Storz Laboratory
SK3281	SK4137 (Δ sibAB/ Δ ibsAB) Δ sibC/ Δ ibsC:: <kan< td=""> <td>This study</td> </kan<>	This study
SK3282	SK4138 (Δ sibAB/ Δ ibsAB <i>rnpA49</i>) Δ sibC/ Δ ibsC:: <kan< td=""> <td>This study</td> </kan<>	This study
SK3283	SK4139 (Δ sibAB/ Δ ibsAB <i>rnc-14</i>) Δ sibC/ Δ ibsC:: <kan< td=""> <td>This study</td> </kan<>	This study

SK3284	SK1647 (<i>ΔsibAB/ΔibsAB rne-1</i>) <i>ΔsibC/ΔibsC::kan</i>	This study
SK3285	SK3281 (<i>ΔsibABC/ΔibsABC</i>)/ pMRK3 (<i>sibC</i>)	This study
SK3286	SK3282 (<i>ΔsibABC/ΔibsABC rnpA49</i>) /pMRK3 (<i>sibC</i>)	This study
SK3287	SK3283 (<i>ΔsibABC/ΔibsABC rnc-14</i>)/ pMRK3 (<i>sibC</i>)	This study
SK3288	SK3284 (<i>ΔsibABC/ΔibsABC rne-1</i>)/ pMRK3 (<i>sibC</i>)	This study
SK3315	SK3281 (<i>ΔsibABC/ΔibsABC</i>) / pMRK3 (<i>sibC</i>) pMRK6 (<i>ibsC</i>)	This study
SK3316	SK3282 (<i>ΔsibABC/ΔibsABC rnpA49</i>)/ pMRK3 (<i>sibC</i>) pMRK6 (<i>ibsC</i>)	This study
SK3317	SK3283 (<i>ΔsibABC/ΔibsABC rnc-14</i>)/ pMRK3 (<i>sibC</i>) pMRK6 (<i>ibsC</i>)	This study
SK3318	SK3284 (<i>ΔsibABC/ΔibsABC rne-1</i>)/ pMRK3 (<i>sibC</i>) pMRK6 (<i>ibsC</i>)	This study
SK3319	SK3281 (<i>ΔsibABC/ΔibsABC</i>)/ pMRK6 (<i>ibsC</i>)	This study
SK3320	SK3282 (<i>ΔsibABC/ΔibsABC rnpA49</i>) / pMRK6 (<i>ibsC</i>)	This study
SK3321	(<i>ΔsibABC/ΔibsABC rnc-14</i>)/ pMRK6 (<i>ibsC</i>)	This study
SK3322	SK3284 (<i>ΔsibABC/ΔibsABC rne-1</i>)/ pMRK6 (<i>ibsC</i>)	This study
SK3727	<i>rneΔ1018::bla thyA715 rph-1 hfq-1::Ω</i> / pBSK1 (<i>rne+</i>)	This laboratory
SK4137	SK1644 no kanamycin, no pCP20	This study
SK4138	SK1645 no kanamycin, no pCP20	This study
SK4139	SK1646 no kanamycin, no pCP20	This study
SK4146	MG1693 <i>ΔsibAB/ΔibsAB ::kan</i>	This study
SK4147	SK2525 (<i>rnpA49</i>) <i>ΔsibAB/ΔibsAB ::kan thyA715 rph-1</i>	This study
SK4148	SK4455 (<i>rnc-14</i>) <i>ΔsibAB/ΔibsAB ::kan thyA715 rph-1</i>	This study
SK4149	SK5665 (<i>rne-1</i>) <i>ΔsibAB/ΔibsAB ::kan thyA715 rph-1</i>	This study
SK4165	SK1647 no kanamycin, no pCP20	This study

SK4455	<i>rnc-14 thyA715 rph-1</i> Tc ^R	(37)
SK5665	<i>rne-1 thyA715 rph-1</i>	(38)
SK9971	<i>rneΔ1018::bla thyA715 rph-1/pMOK16 (rneΔ374 Km^R)</i>	(18)
SK10246	<i>hfq-10 thyA715 rph-1</i> Cm ^R	(35)
Plasmids	Genotype	Source of reference
pCP20	Flp recombinase gene (Cm ^R and Ap ^R)	(13)
pMRK3	single copy plasmid with <i>sibC</i> (Ap ^R)	This study
pMRK6	6-8 copy plasmid with <i>ibsC</i> (Cm ^R)	This study
pMRK7	single copy plasmid with <i>sibC111</i> (Ap ^R)	This study
pMRK9	6-8 copy plasmid with <i>rneΔ374</i> (Sm ^R /Sp ^R)	This study

Table 2.2. Oligos used in this study

Oligo name	Purpose	Sequence
sibC_BamHI	Cloning of sibC	5' CTACCCGGATGATGACGGATCCCCGGTGGTGGTATGGCACA 3'
Bnrr-sibC	Cloning of sibC	5' AGCGGATTTGAACGTTGCGATGGGGCTGTAACGGTAAAGC 3'
Bnrr_end2start	Cloning of sibC	5' TCGCAACGTTCAAATCCGCTCCCGGCGGATTTGTCCTACT 3'
Bnrr_ClaI	Cloning of sibC	5' CATGCGTAGCTAGGGAAGTCCAGGCA 3'
pBMK_BamHI	Cloning of ibsC	5' CGTAGAGGATCCCAGCTGGCAC 3'
pBMKibsC_R	Cloning of ibsC	5' GTATGATGACAAGTCGCATATTTAGATCCTCCTGTTTGAAATTGTTATC 3'
pMRKibsC_F	Cloning of ibsC	5' GGATAACAATTTCAAACGCAGCATGGGGCTGTAACG 3'
ibsC_HindIII	Cloning of ibsC	5' CTAATTTAGAAGCTTAGGGTAAGGGAGGATTGCTCCT 3'
Brrn_ibsC_R	Cloning of ibsC	5' AGCGGATTTGAACGTTGCGAAGGGTAAGGGGAGGATGCTCCT 3'
pMRK_Brrn_R	Cloning of ibsC	5' CATGCGSTCGATGGGAAGTCCAGGC 3'
pMRK7-1_R	Cloning of sibC111	5' GCGTCTCTTTTCTGGAATTAGGAGAAGGGTTATGATGCGA 3'
pMRK7-2_F	Cloning of sibC111	5' TCGCATCATAACCCTTCTCCTAATTCCAGAAAAGAGACGCT 3'
pMRK7-3_R	Cloning of sibC111	5' AGCGGATTTGAACGTTGTAAAGCAACTGGACGAG 3'
pMRK7-4_F	Cloning of sibC111	5' CTCGTCCAGTTGCTTTACAACGTTCAAATCCGCT 3'
sibC_North_1	Probe for Northern	5' TCAGTCTCAGGGGAGGAGCAAT 3'
ibsC_North_1	Probe for Northern	5' ATTGCTCCTCCCCTGAGACTGA 3'

Table 2.3. SibC half-lives in the presence and absence of *ibsC* expression.

Genotype	Half-life (min) ^a	
	<i>sibC/ibsC</i>	Δ <i>sibABC</i> / Δ <i>ibsABC</i> pMRK3 (<i>sibC</i>)
wild-type	9.0 ± 0.3	7.0 ± 0.8
<i>rnpA49</i>	6.3 ± 0.4	6.3 ± 0.6
<i>rnc-14</i>	7.2 ± 0.4	6.3 ± 0.7
<i>rne-1</i>	12.6 ± 1.3	> 20 min
<i>rne-1 rnc-14</i>	8.4 ± 0.2	N.D.

^a Represents the average of at least two independent half-life determinations.

N.D. Not determined.

Table 2.4. SibC half-lives in *hfq* mutants.

Genotype	Half-life (min)^a
wild-type	9.0 ± 0.3
<i>rne-1</i>	12.6 ± 1.3
<i>rne</i> Δ374	4.6 ± 0.3
<i>hfq-10</i>	5.5 ± 0.4
Δ <i>sibABC/ibsABC hfq-10</i> / pMRK3 (sibC)	6.4 ± 1.2
<i>rne</i> Δ1018::bla <i>hfq-1</i> / pMRK9 (<i>rne</i> Δ374)	3.4 ± 0.6
<i>rne-1 hfq-10</i>	25.4 ± 6.3
Δ <i>sibABC/ΔibsABC rne-1 hfq-10</i> / pMRK3 (sibC)	35.2 ± 3.5
<i>rnc-14</i>	7.2 ± 0.4
<i>rnc-14 hfq-10</i>	3.8 ± 0.4
Δ <i>sibABC/ΔibsABC rnc-14 hfq-10</i> / pMRK3 (sibC)	9.6 ± 0.7

^a Represents the average of at least two independent half-life determinations.

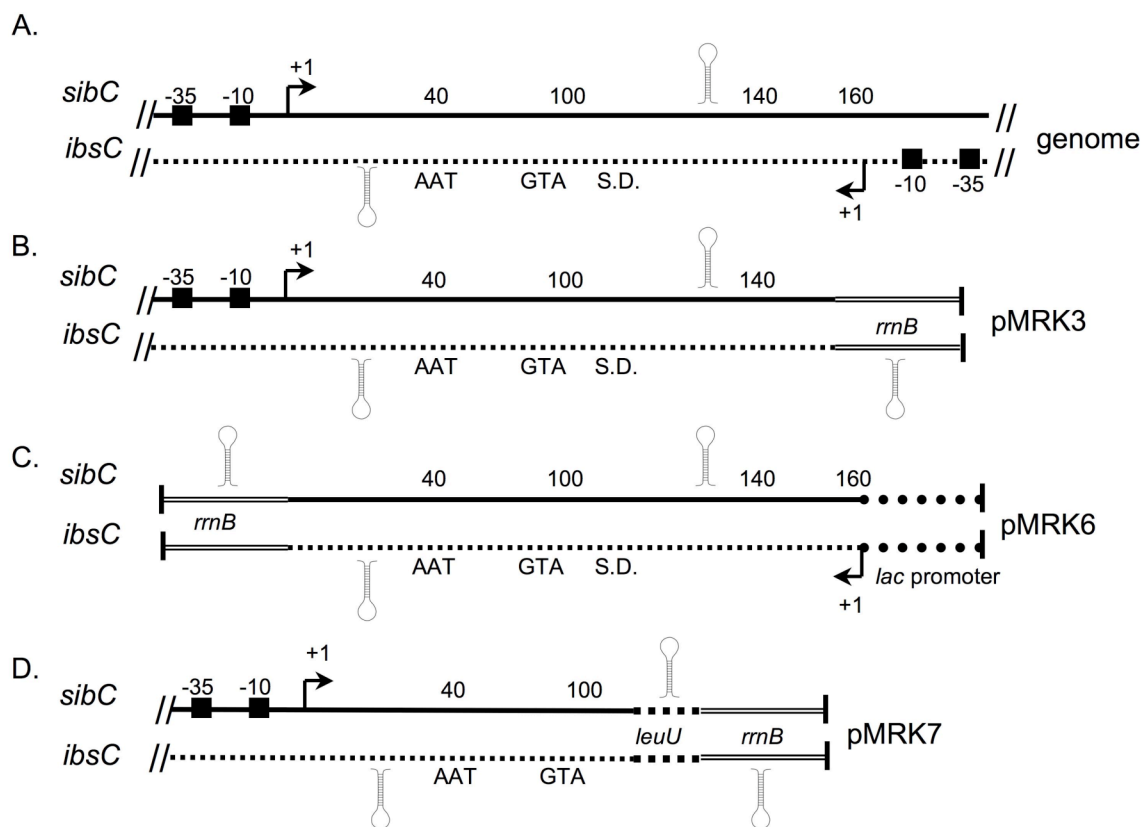


Figure 2.1. Description of the *SibC* and *IbsC* plasmids used in this study.

A. Schematic of the *SibC* (top strand) and *IbsC* (bottom strand) locus of the *E. coli* genome. The -10 and -35 regions are represented by black boxes and transcription start sites by arrows. The Shine-Delgarno (S.D) sequence and the start and stop codons of *ibsC* are labeled. The stem-loop structures represent inverted repeats that could potentially terminate transcription. B. Schematic of pMRK3. The first 154 nucleotides of *SibC*, including the inverted repeat that could act as a terminator, along with approximately 500 bp upstream of the promoter, were cloned into a single-copy plasmid as described in *Materials and methods*. The promoter region of *ibsC* was omitted and the *rrnB* terminator was cloned in the opposite strand. C. Schematic of pMRK6. The *IbsC* transcript without its promoter was placed in front of the *lac* promoter. The inverted repeats that could act as terminators were included, but the promoter of *SibC* was not. In addition, an *rrnB* terminator was cloned at the 5' of *SibC* to prevent its expression. D. Schematic of pMRK7. This plasmid has the same 5' as pMRK3, but it only contains the first 112 nucleotides *sibC*, after which the *leuU* terminator was placed. The *rrnB* terminator was placed in the opposite strand to prevent *ibsC* expression.

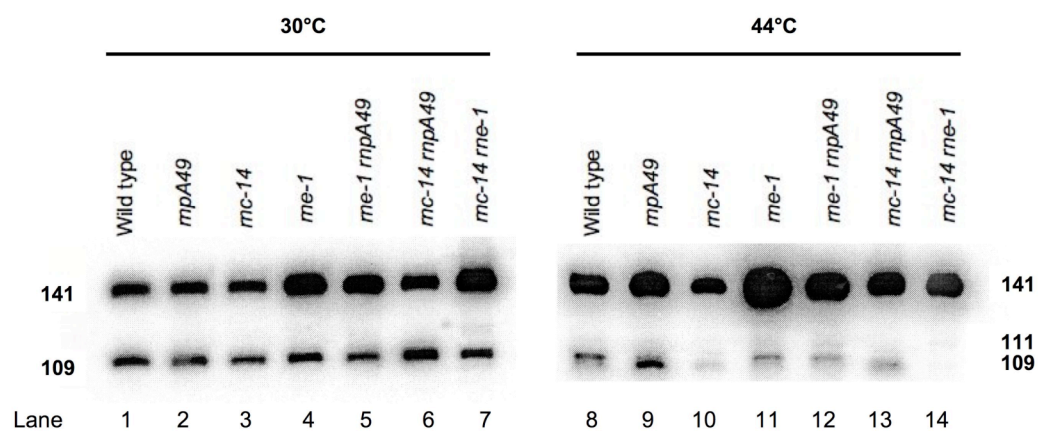


Figure 2.2. Steady-state analysis of SibC in early-stationary phase cultures at 30°C and 44°C. Sizes were estimated based on electrophoretic mobility using a RiboRuler low range RNA ladder (Fermentas) and they are in agreement to what was previously reported by Fozo *et al.* (2008).

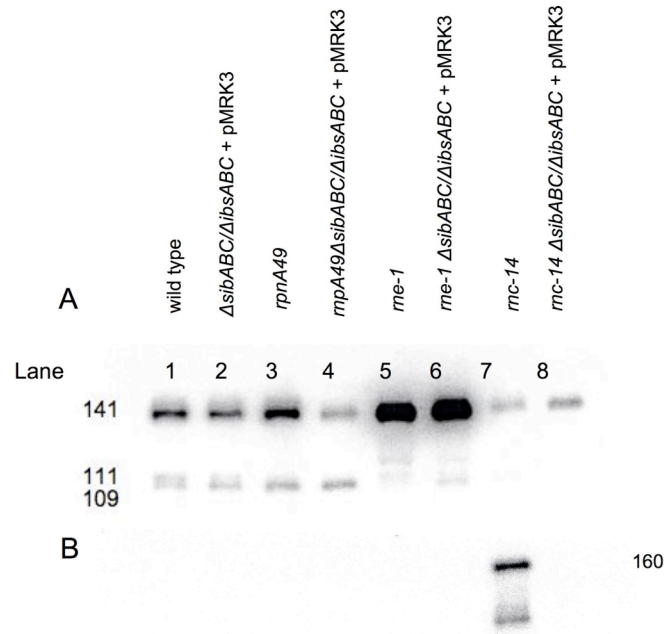


Figure 2.3. Steady-state analysis of SibC and *ibsC* at 44°C. A. Membrane probed for SibC. B. Same membrane as panel A, stripped and reprobbed for *ibsC*. Sizes were estimated based on electrophoretic mobility using a RiboRuler low range RNA ladder (Fermentas).

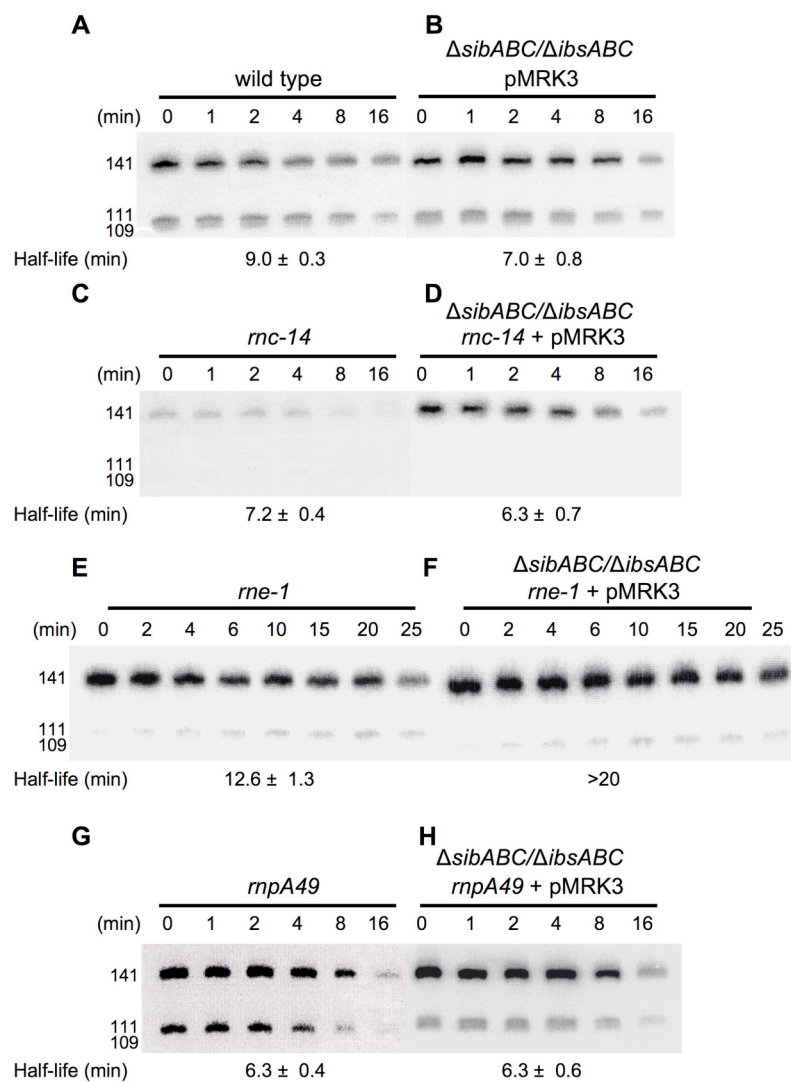


Figure 2.4. Half-lives of SibC141 in the presence and absence of its target, *ibsC*. Data represent the average of at least two independent determinations. Sizes were estimated based on electrophoretic mobility using a RiboRuler low range RNA ladder (Fermentas).

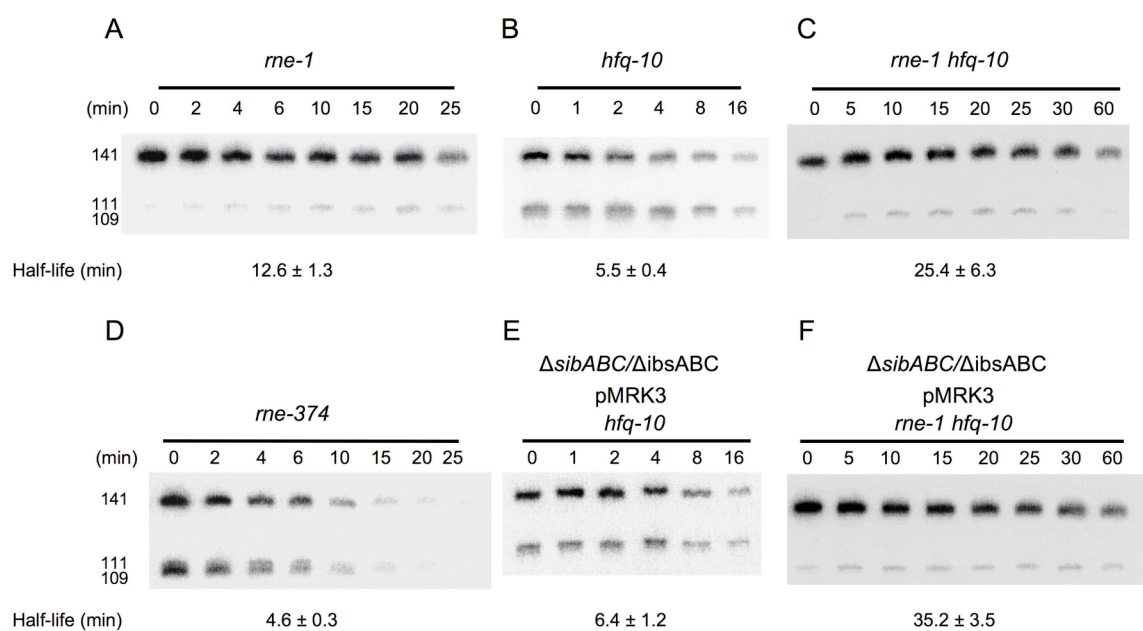


Figure 2.5. Half-lives of SibC141 in RNase E and Hfq mutants. Data represent the average of at least two independent determinations. Sizes were estimated based on electrophoretic mobility using a RiboRuler low range RNA ladder (Fermentas).

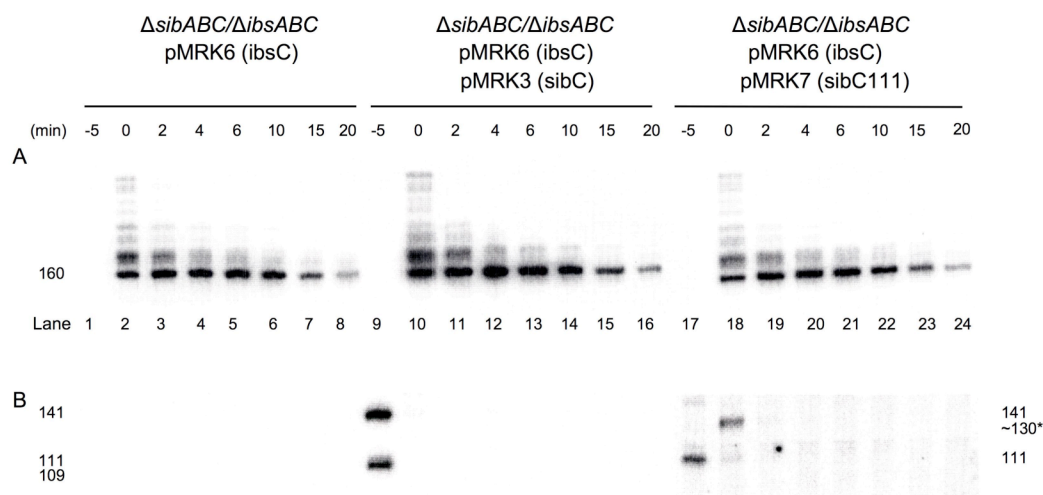


Figure 2.6. Half-lives of *ibsC*. First time point (-5) was collected prior to *ibsC* induction. IPTG was added and, after a 5 minutes induction, rifampicin was added. Time point 0 was collected after 80 seconds after the addition of rifampicin and at the indicated times thereafter. A. Membranes probed for *ibsC*. B. Same membranes as panel A stripped and reprobed for SibC. Sizes were estimated based on electrophoretic mobility using a RiboRuler low range RNA ladder (Fermentas). The asterisk (*) denotes the presence of a new band of unknown origin.

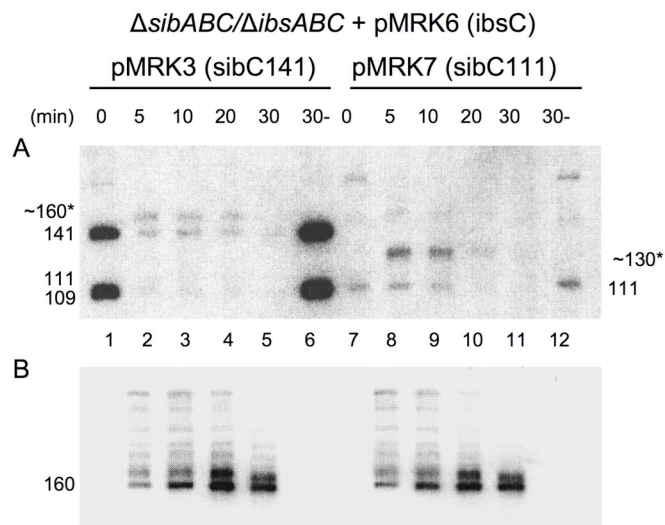


Figure 2.7. SibC processing after *ibsC* induction. Samples were collected at the indicated times after IPTG addition. A. Membrane probed for SibC. B. Same membrane stripped and reprobbed for *ibsC*. Sizes were estimated based on electrophoretic mobility using a RiboRuler low range RNA ladder (Fermentas). The asterisks (*) denote the presence of new bands of unknown origin.

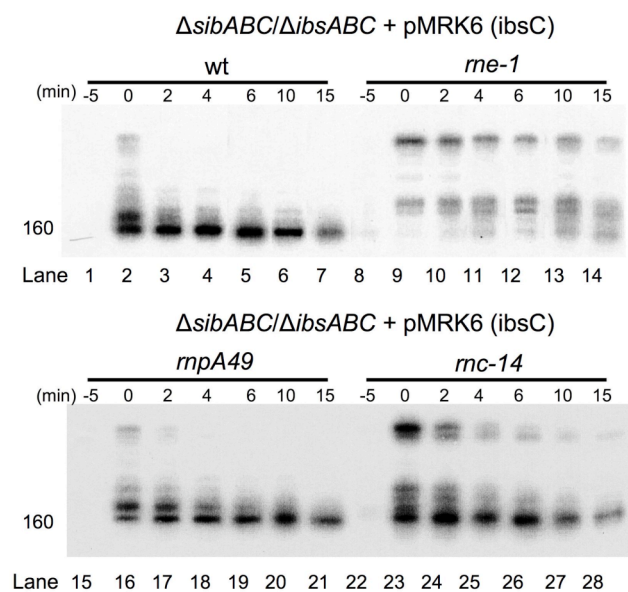


Figure 2.8. *IbsC* processing in the absence of SibC. First time point (-5) was collected before *ibsC* induction. IPTG was added and, after a 5 minutes induction, rifampicin was added. Time point 0 was collected after 80 seconds after the addition of rifampicin and at the indicated times thereafter. Sizes were estimated based on electrophoretic mobility using a RiboRuler low range RNA ladder (Fermentas).

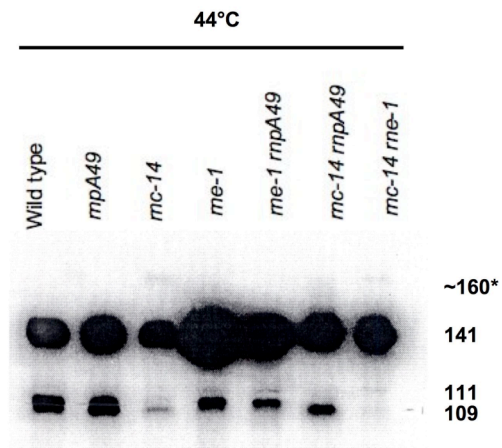


Figure S.2.1. Overexposed Northern blot of SibC shown in Figure 2.2. The asterisk (*) denotes the presence of a new band of unknown origin.

CHAPTER 3

THE MRNA INTERFERASE ENCODED BY MAZF DOES NOT PLAY A ROLE IN
MRNA DECAY IN *ESCHERICHIA COLI*¹

¹ Roche Ríos, Marly I. and Kushner, Sidney R. To be submitted to *Journal of Bacteriology*.

ABSTRACT

The *mazF* gene of *Escherichia coli* encodes an endoribonuclease that cleaves mRNAs at ACA trinucleotides. The mRNAs do not have to be associated with ribosomes to undergo cleavage. The *mazF* gene is part of a toxin-antitoxin system whose expression is induced by various stress conditions including inhibition of transcription by rifampicin and DNA damage. Here we have examined if the presence of the MazF endonuclease affects the measurement of mRNA half-lives, since transcription initiation is inhibited in these measurements by the addition of rifampicin. Surprisingly, deletion of MazF did not lead to any change in the half-lives of two transcripts (*rpsO* and *cspE*) that contain multiple MazF cleavage sites. However, we did observe that deletion of MazG, a gene that helps regulate the stringent response, led to significant alterations in mRNA half-lives.

INTRODUCTION

Toxin-antitoxin (TA) modules in bacteria were first identified in the 1980s in plasmids, where they are involved in plasmid maintenance (1), by helping to control post-segregational killing. TA systems are organized in operons and consist of a labile antitoxin encoded upstream of a stable toxin. If a daughter cell does not inherit the plasmid after cell division, the antitoxin levels rapidly decrease, allowing the more stable toxin to function, killing the cells that did not inherit the plasmid (2,3). Homologs of these toxin-antitoxin systems have also been identified in the *E.coli* chromosome and they have been found in most free-living bacteria (4,5). Although their chromosomal role is still the subject of great debate, evidence indicates that many TA systems are involved in various stress response mechanisms (6,7). Stressful conditions such as DNA damage, nutrient starvation, and certain antibiotics prevent the expression of the antitoxins, leading to the activation of toxin proteins that cause growth inhibition and/or cell death (8,9) [reviewed in (7,10)].

Based on antitoxin similarities, five types of toxin-antitoxin families have been defined so far. Most of the characterized toxins exert their toxic effect by either interfering with the activity of DNA gyrase or by cleaving mRNA (10). The most extensively studied toxins thus far are RelB and MazF. These two enzymes belong to the type II TA systems family and they act by inhibiting translation (11). While RelB induces mRNA cleavage on the A site of a translating ribosome, MazF cleaves ACA sequences in the mRNA independently of translation (9,12). Their toxic effects are neutralized by the formation of protein-protein complexes with their respective antitoxic peptides (11).

Endoribonucleases like MazF, with the ability to cleave mRNAs at specific nucleotide sequences, have been termed “mRNA-interferases” [reviewed in (13)].

The *mazEF* TA system was the first chromosomal so called “addiction module” to be described in *E.coli*. It is part of the *rel* operon, with the *relA* gene located upstream and *mazG* downstream (8,14). *relA* encodes an enzyme required for guanosine 3',5'-bispyrophosphate (ppGpp) synthesis, a major regulator of the stringent response, which is induced in response to amino acid starvation. ppGpp was also shown to inhibit transcription of the *mazEF* operon (8). MazG encodes a nucleotide pyrophosphohydrolase that can lower the levels of ppGpp in the cell and therefore inhibit the induction of the stringent response. Interestingly, the enzymatic activity of MazG is greatly inhibited in the presence of MazEF. Gross *et al.* (15) proposed a model in which MazG also plays a role in MazEF-mediated cell death. As a result of nutritional stress, ppGpp levels go up, inhibiting transcription of the *mazEF* operon. The remaining MazE protein in the cell is degraded by proteases, freeing MazF from its antitoxin. In turn, degradation of MazE releases the repression the *mazEF* complex has on MazG activity, allowing MazG to deplete the pool of ppGpp, shutting down the stringent response and permitting new transcription of the *mazEF* operon.

Although none of the mRNA interferases have been implicated in general mRNA decay in *E. coli*, we decided to determine if the MazF endoribonuclease affected the determinations of mRNA half-lives, since their measurement involves the addition of rifampicin and nalidixic acid to the bacterial cultures. As an inhibitor of transcription, rifampicin prevents the continuous expression of the antitoxin, MazE, allowing MazF to

act freely and leading to *mazEF*-mediated cell death (16). Furthermore, nalidixic acid acts as a DNA damaging agent by inhibiting a subunit of DNA gyrase, an event that has also been shown to trigger *mazEF*-mediated cell death (17). Therefore, we hypothesized that the measurement of mRNA half-lives in *E.coli* leads to MazF endoribonuclease induction, possibly resulting in altered half-life determinations. We predicted that activation of MazF would lead to shorter mRNAs half-lives, particularly for those transcripts that contain MazF cleavage sites (ACA sequences). Here we show that in the MG1693 genetic background, there were no differences in the half-lives of the *rpsO* and *cspE* mRNAs in the presence or absence of *mazEFG*. However, in the W3110 background both messages actually become less stable when all three *maz* genes, *mazE*, *F*, and *G*, were absent. This surprising result appeared to be related to the deletion of *mazG*, because when *mazF* was deleted by itself, the mRNAs no longer exhibited increased stability. The differential response to the *mazG* deletion observed in MG1693 and W3110 genetic backgrounds warrants further investigation, as it could be attributed to any of the many variations in their gene content (35).

MATERIALS AND METHODS

Strain construction

Strains used in this study are listed in Table 3.1. For the construction of *mazEFG* deletions strains, a P1 lysate grown on the MC4100 Δ *mazEFG::kan* strain, provided by the Kolodkin-Gal laboratories, was used for transductions (8). Kan^R transductants were first tested for the presence of the *mazEFG* deletion via PCR using primers *mazEF* 5' and *mazG*. The *rne-1* mutation (18) was moved into the W3110 background via a two-step

transduction. First, a P1 lysate grown on SK5664 was used to introduce the *pyrC::Tn10* allele to generate SK4134. This strain was then transduced with lysate grown on SK5665 (*rne-1*). Since the *rne-1* allele is cotransductionally linked to *pyrC*, transductants were selected by their ability to grow on minimal medium. Subsequently, temperature sensitivity at 44°C was used to confirm the presence of the *rne-1* allele. Strains deleted for *mazF* alone were constructed by transduction using a P1 lysate grown on JW2753 (*chpA781::kan*) obtained from the Keio collection at the *E.coli* Genetic Stock Center (19). *mazF* was originally designated *chpA*. Deletions were confirmed via PCR with primers *mazEF* 5' and *mazEF* 3'. RNase Z deletion strains were constructed by P1 transduction using phage grown on SK4477 (Δ *rnz::apr*) and were confirmed using PCR with *elaC*-sense and *elaC*-antisense primers. All primers are used in these experiments are listed in Table 3.2.

Growth conditions

Bacterial strains were grown into exponential phase (Klett 50, as measured by a Klett-Summerson colorimeter with a green filter, no. 42) in Luria broth supplemented with thymine (50 µg/ml) and the appropriate antibiotic for selection. For growth curves, strains were subsequently switched to 44°C and kept at ~75 Klett units above background by diluting the cultures with pre-warmed medium. Measurements were taken every 30 min. Strains used for half-life calculations were grown at 30°C to ~50 Klett units above background, switched to 44°C after the addition of 500 µg/ml of rifampicin and 20 µg/ml of nalidixic acid, and samples collected at specified times.

RNA isolation

RNA was extracted from exponentially growing cells using a modified version of the method previously described by O'Hara *et al.*(20). Briefly, cultures were added to TM crushed-ice buffer with a final concentration of 10 mM Tris pH 7.2, 5 mM magnesium chloride, 20 mM sodium azide, 0.4 mg/ml chloramphenicol and spun down. Cell pellets were resuspended in lysis buffer [12 μ L of 10 mg/mL of lysozyme (Sigma) and 1.3 μ L of RNase-free DNase I (Roche) per mL of TM buffer] and snap frozen in a dry ice/ethanol bath. Acetic acid was added to the frozen lysis solution and three freeze/thaw cycles were done at 37°C. After the last thaw, an equal volume of 10% trimethyl(tetradecyl) ammonium bromide (Sigma) was added and the cells were centrifuged 5,000 rpm for 5 min at 4°C. Pellets were resuspended in a 2 M lithium chloride solution in 35% ethanol. The samples were centrifuged for 6 minutes at 4°C and the pellets were then resuspended in a 2 M lithium chloride solution in water, incubated for 5 minutes at room temperature, and centrifuged again. The pellets were rinsed in 70% ethanol, dried, and resuspended in RNase-free water. RNA was quantified using a Nanodrop 2000c (Thermo Scientific).

Northern Blotting

For mRNA half-life determinations, samples were taken after the addition of rifampicin and nalidixic acid to a final concentration of 500 μ g/ mL and 20 μ g/ mL, respectively. Ten μ g of total RNA were mixed with an equal volume of Gel loading Buffer II (Ambion) and resolved on 6%/7M urea polyacrylamide gels in 1X TBE. RNA was transferred overnight at 10V to Nytran SPC membranes (Whatman) at 4°C and 1 hour at 40V. Membranes were subsequently baked at 80°C for 30 minutes and UV cross-linked.

for 20 seconds. Before probing, membranes were washed in 2% SCC and incubated in PerfectHyb buffer (Sigma) at 65°C. Strippable probes were generated by randomly labeling message-specific PCR products with ³²P- α -ATP using α -thiol CTP and Klenow enzyme (NEB). Primers used are listed on Table 3.2. Membranes were exposed to phosphor screens and scanned using a Storm 840 Phosphorimager (GE Healthcare). Band intensities were determined using ImageQuant 5.2 software (GE Healthcare). Linear regression analyses were used to calculate the mRNA half-life.

RESULTS

Analyzing the role of the *mazF* encoded endoribonuclease in general mRNA decay

The *mazF* encoded endoribonuclease cleaves at ACA sequences in mRNA (12). Previous experiments performed to identify *mazEF*-mediated cell death inducers showed that concentrations of 15-25 μ g/ml of rifampicin and 2 mg/ml of nalidixic acid were sufficient to trigger killing (16,17). Since standard protocols for determining mRNA half-lives involve the addition of 500 μ g/ml of rifampicin and 20 μ g/ml of nalidixic acid, we wanted to determine if the results of such determinations were altered by the induction of the MazF endoribonuclease. To test this hypothesis, we chose two well-characterized transcripts, *rpsO* and *cspE* (21,22,23,24) that contain multiple ACA sequences (*rpsO*, 30 sites; *cspE*, 7 sites) for detailed analysis. Furthermore, both of these transcripts have been shown to be substrates for RNase E (24-26), the primary endoribonuclease involved in *E.coli* mRNA decay (27,28). Accordingly, we constructed a series of strains that carried the temperature sensitive *rne-1* allele (29) as well as a *mazEFG* deletion.

In the MG1693 background, the half-life of *rpsO* was 3.8 min in the *rne-1* strain compared to 1.4 min in the wild-type control (Figure 3.1). This result was in agreement

with previous published work (30). Surprisingly, no difference in the *rpsO* half-life was observed between the single *rne-I* mutant and the *rne-I* Δ *mazEFG* multiple mutant (3.5 min, Figure 3.1). However, Kolodkin-Gal and Engelberg-Kulka (2008) had shown that MG1655 was five times more resistant to *mazEF*-mediated toxicity when compared to W3110, MC4100, and K38 *E.coli* strains, even though MG1693 contains both MazE and MazF (31). Although MG1655 and W3110 have the same chromosome size, W3110 is missing 82 of the ORFs found in MG1655 and has approximately 65kb of novel sequences not found in MG1655 (35). Thus, it was possible that the lack of a *mazF* effect was related to some unique property of the MG1655 genetic background (MG1693 is a *thyA715* derivative of MG1655).

To test this possibility, we constructed *rne-I* and *rne-I* Δ *mazEFG* mutants in the W3110 genetic background (Table 3.1). The W3110 mutant strains showed the same growth properties as their MG1693 counterparts (Figure 3.2). Subsequently, we determined the half-lives of both, *rpsO* and *cspE*. Interestingly, the half-life of *rpsO* was longer in the *rne-I* strain in W3110 genetic background (5.4 min, Figure 3.3) compared to MG1693 genetic background (3.8 min, Figure 3.2). Surprisingly, inactivating *mazEFG* in an *rne-I* genetic background led to a significantly shorter half-life (3.3 min, Figure 3.3) than in the *rne-I* single mutant. Similar results were obtained with the *cspE* transcript where the half-life in the *rne-I* strain (9.4 min, Figure 3.3) decreased to 6.1 min in the *rne-I* Δ *mazEFG* multiple mutant (Figure 3.3).

Relationship of RNase Z and MazEFG in mRNA decay

MazF induction leads to a general inhibition of protein synthesis as a result of multiple mRNA cleavages (12). However, Amitai *et al.*(32) identified a group of proteins

that were selectively synthesized after MazF induction. In fact, one of the proteins showing increased levels of synthesis after MazF induction was the product of the *elaC/rnz* gene, which was shown to encode RNase Z, an endoribonuclease that has been demonstrated to be involved in general mRNA decay (24). RNase Z has been shown to be required for the maturation of tRNA precursors that lack the encoded 3' CCA terminal sequence (33). However, since *E.coli* tRNA genes carry an encoded terminal CCA sequence, this function of RNase Z is not needed (34). Rather, Perwez and Kushner (2006) showed that in *E.coli* RNase Z plays a role in mRNA decay pathways, particularly for the *cspE* mRNA. It was thus possible that the decrease in the *rpsO* and *cspE* half-lives resulted from increased levels of RNase Z.

To test this hypothesis, we constructed an *rne-1 ΔmazEFG Δrnz* triple mutant in the W3110 genetic background and determined the *rpsO* and *cspE* mRNA half-lives. As shown in Figure 3.3, the half-life of the *rpsO* mRNA was slightly longer in the triple mutant (4.3 min) compared to the *rne-1 ΔmazEFG* double mutant (3.3 min). However, in the case of *cspE*, the half-life decreased from 6.1 min (*rne-1 ΔmazEFG*) to 4.2 min (*rne-1 ΔmazEFG Δrnz*). This result was in contrast to a half-life of 12.1 min in the *rne-1 Δrnz* double mutant (Table 3.3).

Role of MazG in message stability

The *mazEF* operon also includes the downstream gene *mazG*, which encodes a nucleotide pyrophosphohydrolase (14). MazG has been shown to lower the levels of (p)ppGpp in the cells, helping prevent the induction of the stringent response in nutritionally starved cells (15). Since deletion of *mazG* would lead to increased levels of ppGpp and persistence of the stringent response, it was possible that the decreased half-

lives observed in the *ΔmazEFG* strains were unrelated to the MazF endoribonuclease but rather were associated with the induction and persistence of the stringent response. To test this possibility we constructed a new set of strains in which the *mazF* coding sequence was deleted. As shown in Table 3.4, the half-lives of the *rpsO* and *cspE* mRNAs were identical, within experimental error in the *rne-1* and *rne-1 ΔmazF* strains. Furthermore the increase in the half-life of the *cspE* mRNA in the *rne-1 Δrnz* double mutant was comparable to what was obtained in the *rne-1 ΔmazF Δrnz* triple mutant (Tables 3.3 and 3.4). It should be noted that it has previously been shown that the half-life of *cspE* mRNA is significantly affected by the inactivation of RNase E (24). These results would suggest that the effect of mRNA half-life observed in the *ΔmazEFG* deletion was related to the inactivation of MazG rather than MazF.

DISCUSSION

We have shown here for the first time that the MazF endoribonuclease does not play a role in general mRNA decay in *E.coli* in either the MG1693 or W3110 genetic backgrounds. In the MG1693 genetic background, deleting *mazEFG* in an *rne-1* strain had no effect in the half-life of *rpsO* (Figure 3.1). Interestingly, the same deletion in the W3110 background resulted in shorter *rpsO* and *cspE* half-lives (Figure 3.3, Table 3.2). Data published by Kolodkin-Gal and Engelberg-Kulka (31) could explain these differences in MazF activity. They reported strain background differences in *mazEF*-mediated cell death. MG1655 is defective in EDF production and response when compared to W3110, K38 and MC4100 strains. Since, EDF is a small peptide required for *mazEF*-mediated cell death, MG1655 is resistant to deleterious effect of this TA module. Even though these strain differences are not well understood, they could explain

the difference in MazF activity between the strains. Furthermore, W3110 is estimated to have 65Kb of unique DNA relative to MG1655 and it is missing 82 of the ORFs found in MG1655 (35). Any one of these genes could be responsible for the differences observed between strains.

We also ruled out RNase Z as a possible candidate to explain the observed decrease in mRNA half-life. Amitai *et al.* (32) identified a group of small proteins whose levels go up after MazF induction. Among these proteins was RNase Z. RNase Z is one of the enzymes responsible for the 3' end maturation of tRNAs in species lacking the terminal CCA sequence (33). However, all *E.coli* tRNAs genes carry an encoded 3' CCA. We have previously reported that RNase Z plays a significant role in mRNA decay in *E.coli* (24). Data from a macroarray used to compare steady-state levels from a genome-wide analysis showed an increase in the steady-state levels of more than 150 mRNAs in a strain harboring a chromosomal deletion of *rnz* as compared to wild-type (24). Northern analysis confirmed that in an *rnz rne-1* double mutant strain, all 5 half-lives studied increased compared to the wild-type control and to the *rne-1* and *rnz* single mutants. The stability increases observed were not mediated via changes in RNase E levels, since the *rnz* deletion did not affect its protein levels in the cell (24). Here we showed that adding the *rnz* deletion to the *rne-1 ΔmazEFG* mutant strain did not increase the half-life of either transcript as would be expected if RNase Z was responsible for the decrease in mRNA half-life after MazF induction in the W3110 genetic background (Table 3.3).

Surprisingly, our data suggest that the decrease in mRNA half-life observed in the *rne-1 ΔmazEFG* strains in the W3110 genetic background is directly related to MazG

activity, not MazF since we observed no differences in mRNA half-lives between the *rne-1* and the *rne-1* $\Delta mazF$ strains. These results would indicate that MazF does not play a role in general mRNA decay and suggest a possible role for MazG in message stability.

Under conditions of nutrient starvation, RelA synthesizes (p)ppGpp, an alarmone that redirects the cellular machinery to decrease rRNA and tRNA synthesis and increase biosynthetic pathways and transcription of stress-related genes to allow the cells to survive the stress (36). In addition to RelA, SpoT has been shown to synthesize (p)ppGpp, although not as effectively (37). SpoT also contains a hydrolase activity that allows it to degrade (p)ppGpp, inhibiting the stringent response and restoring the cells normal function (38,39). MazG was recently also described as nucleotide pyrophosphohydrolase with the ability to turnover ppGpp (14,15). By lowering the cellular levels of ppGpp, MazG can also regulate *mazEF* expression (15). ppGpp has been shown to prevent transcription of the MazEF operon, which would decrease the levels of MazE and, in turn, lead to MazF activation. In the absence of either SpoT and/or MazG, ppGpp levels would accumulate in the cell, which could result in prolonged MazF activity and persistence of the stringent response.

RNase E plays a crucial role in tRNA processing events required for 3' end maturation (40). It is therefore possible that in *rne-1* mutants, the stringent response is induced, and that deleting MazG disrupts its regulation.

Durfee *et al.* (41) looked at gene expression profiles after inducing the stringent response with serine hydroxymate treatment (SHX). Five minutes after treatment, they saw downregulation of 27 genes and upregulation of 83 genes. Among the downregulated genes were several genes involved in flagellum synthesis, *fis*, a positive transcriptional

regulator of rRNA operons(42), *rnpA*, the protein component of RNase P, *holA*, the delta subunit of DNA polymerase III, as well as several genes involved in nucleotide biosynthesis (*pyrF*, *pur*, and *apt*) (42). When we looked at transcription changes in *rne-1* strains as compared to wild-type in the MG1693 background, we also observed a significant downregulation in *rnpA*, *holA*, *fis*, and *pyrF*. Although the flagellar genes were up-regulated in the *rne-1* mutant, many of the genes repressed after stringent response induction were also down-regulated in *rne-1* strain (K. Mildenhall and S. Kushner, unpublished results).

In addition, we observed great similarity in the up-regulation of gene expression between the *rne-1* and SHX treated cells. Genes like *rpoE*, *rpoH*, and *rsd*, involved in transcriptional regulation were up-regulated in both cases. Non-sigma transcription factors, such as *lexA*, *crp*, *bolA*, *phoB*, *pspB*, and *lrp* were also up-regulated in *rne-1* mutants as well as SHX treated cells (41) (K. Mildenhall and S. Kushner, unpublished results). These similarities support the hypothesis that inactivation of RNase E could induce the stringent response.

However, our data shows the potential induction of the stringent response by *rne-1* in the MG1655 background, where deleting MazG had no effect in the mRNA half-life of *rpsO*. Although we have not looked at the transcription profile of the *rne-1* strain in the W3110 genetic background, the lack of growth differences between the *rne-1* in MG1693 and *rne-1* in W3110, would suggest that both strains are being equally affected by the RNase E deficiency of the *rne-1* allele (Figure 3.2). The question still remains, why does MazG have an effect in mRNA half-lives in the W3110 background, but not in

the MG1693 background. It would also be interesting to analyze further the effect of *rne-1* in the stringent response, as well as the role of MazG in regulating the response.

ACKNOWLEDGEMENTS

This work was supported in part by a grant from the National Institute of General Medical Sciences to S.R.K.

REFERENCES

1. Ogura, T., Tomoyasu, T., Yuki, T., Morimura, S., Begg, K.J., Donachie, W.D., Mori, H., Niki, H. and Hiraga, S. (1991) Structure and function of the *ftsH* gene in *Escherichia coli*. *Res. Microbiol.*, 142, 279-282.
2. Gerdes, K., Larsen, J.E. and Molin, S. (1985) Stable inheritance of plasmid R1 requires two different loci. *J. Bacteriol.*, 161, 292-298.
3. Gerdes, K., Rasmussen, P.B. and Molin, S. (1986) Unique type of plasmid maintenance function: postsegregational killing of plasmid-free cells. *Proc. Natl. Acad. Sci. U S A*, 83, 3116-3120.
4. Masuda, Y., Miyakawa, K., Nishimura, Y. and Ohtsubo, E. (1993) *chpA* and *chpB*, *Escherichia coli* chromosomal homologs of the *pem* locus responsible for stable maintenance of plasmid R100. *J. Bacteriol.*, 175, 6850-6856.
5. Pandey, D.P. and Gerdes, K. (2005) Toxin-antitoxin loci are highly abundant in free-living but lost from host-associated prokaryotes. *Nucleic Acids Res.*, 33, 966-976.
6. Gerdes, K., Christensen, S.K. and Lobner-Olesen, A. (2005) Prokaryotic toxin-antitoxin stress response loci. *Nat. Rev.*, 3, 371-382.

7. Buts, L., Lah, J., Dao-Thi, M.H., Wyns, L. and Loris, R. (2005) Toxin-antitoxin modules as bacterial metabolic stress managers. *Trends Biochem. Sci.*, 30, 672-679.
8. Aizenman, E., Engelberg-Kulka, H. and Glaser, G. (1996) An *Escherichia coli* chromosomal "addiction module" regulated by guanosine 3',5'-bispyrophosphate: a model for programmed bacterial cell death. *Proc. Natl. Acad. Sci. U S A*, 93, 6059-6063.
9. Christensen, S.K., Mikkelsen, M., Pedersen, K. and Gerdes, K. (2001) RelE, a global inhibitor of translation, is activated during nutritional stress. *Proc. Natl. Acad. Sci. U S A*, 98, 14328-14333.
10. Van Melderen, L. and Saavedra De Bast, M. (2009) Bacterial toxin-antitoxin systems: more than selfish entities? *PLoS Genet.*, 5, e1000437.
11. Gotfredsen, M. and Gerdes, K. (1998) The *Escherichia coli relBE* genes belong to a new toxin-antitoxin gene family. *Mol. Microbiol.*, 29, 1065-1076.
12. Zhang, Y., Zhang, J., Hoeflich, K.P., Ikura, M., Qing, G. and Inouye, M. (2003) MazF cleaves cellular mRNAs specifically at ACA to block protein synthesis in *Escherichia coli*. *Mol. Cell*, 12, 913-923.
13. Inouye, M. (2006) The discovery of mRNA interferases: implication in bacterial physiology and application to biotechnology. *J. Cell. Physiol.*, 209, 670-676.
14. Zhang, J. and Inouye, M. (2002) MazG, a nucleoside triphosphate pyrophosphohydrolase, interacts with Era, an essential GTPase in *Escherichia coli*. *J. Bacteriol.*, 184, 5323-5329.

15. Gross, M., Marianovsky, I. and Glaser, G. (2006) MazG -- a regulator of programmed cell death in *Escherichia coli*. *Mol. Microbiol.*, 59, 590-601.
16. Sat, B., Hazan, R., Fisher, T., Khaner, H., Glaser, G. and Engelberg-Kulka, H. (2001) Programmed cell death in *Escherichia coli*: some antibiotics can trigger *mazEF* lethality. *J. Bacteriol.*, 183, 2041-2045.
17. Hazan, R., Sat, B. and Engelberg-Kulka, H. (2004) *Escherichia coli mazEF*-mediated cell death is triggered by various stressful conditions. *J. Bacteriol.*, 186, 3663-3669.
18. Arraiano, C.M., Yancey, S.D. and Kushner, S.R. (1988) Stabilization of discrete mRNA breakdown products in *ams pnp rnb* multiple mutants of *Escherichia coli* K-12. *J. Bacteriol.*, 170, 4625-4633.
19. Baba, T., Ara, T., Hasegawa, M., Takai, Y., Okumura, Y., Baba, M., Datsenko, K.A., Tomita, M., Wanner, B.L. and Mori, H. (2006) Construction of *Escherichia coli* K-12 in-frame, single-gene knockout mutants: the Keio collection. *Mol. Sys. Biol.*, 2, 2006 0008.
20. O'Hara, E.B., Chekanova, J.A., Ingle, C.A., Kushner, Z.R., Peters, E. and Kushner, S.R. (1995) Polyadenylation helps regulate mRNA decay in *Escherichia coli*. *Proc. Natl. Acad. Sci. U S A*, 92, 1807-1811.
21. Hajnsdorf, E., Braun, F., Haugel-Nielsen, J., Le Derout, J. and Régnier, P. (1996) Multiple degradation pathways of the *rpsO* mRNA of *Escherichia coli*. RNase E interacts with the 5' and 3' extremities of the primary transcript. *Biochimie*, 78, 416-424.

22. Hajnsdorf, E. and Regnier, P. (1999) *E. coli rpsO* mRNA decay: RNase E processing at the beginning of the coding sequence stimulates poly(A)-dependent degradation of the mRNA. *J. Mol. Biol.*, 286, 1033-1043.
23. Delvillani, F., Papiani, G., Deho, G. and Briani, F. (2011) S1 ribosomal protein and the interplay between translation and mRNA decay. *Nucleic Acids Res.*, 39, 7702-7715.
24. Perwez, T. and Kushner, S.R. (2006) RNase Z in *Escherichia coli* plays a significant role in mRNA decay. *Mol. Microbiol.*, 60, 723-737.
25. Ow, M.C., Liu, Q., Mohanty, B.K., Andrew, M.E., Maples, V.F. and Kushner, S.R. (2002) RNase E levels in *Escherichia coli* are controlled by a complex regulatory system that involves transcription of the *rne* gene from three promoters. *Mol. Microbiol.*, 43, 159-171.
26. Ow, M.C., Perwez, T. and Kushner, S.R. (2003) RNase G of *Escherichia coli* exhibits only limited functional overlap with its essential homologue, RNase E. *Mol. Microbiol.*, 49, 607-622.
27. Carpousis, A.J. (2007) The RNA degradosome of *Escherichia coli*: An mRNA-degrading machine assembled on RNase E. *Annu. Rev. Microbiol.*, 61, 71-87.
28. Mackie, G.A. (2012) RNase E: at the interface of bacterial RNA processing and decay. *Nat. Rev. Microbiol.*, 11, 45-57.
29. Babitzke, P. and Kushner, S.R. (1991) The Ams (altered mRNA stability) protein and ribonuclease E are encoded by the same structural gene of *Escherichia coli*. *Proc. Natl. Acad. Sci. U S A*, 88, 1-5.

30. Ow, M.C., Liu, Q. and Kushner, S.R. (2000) Analysis of mRNA decay and rRNA processing in *Escherichia coli* in the absence of RNase E-based degradosome assembly. *Mol. Microbiol.*, 38, 854-866.
31. Kolodkin-Gal, I. and Engelberg-Kulka, H. (2008) The extracellular death factor: physiological and genetic factors influencing its production and response in *Escherichia coli*. *J. Bacteriol.*, 190, 3169-3175.
32. Amitai, S., Kolodkin-Gal, I., Hananya-Meltabashi, M., Sacher, A. and Engelberg-Kulka, H. (2009) *Escherichia coli* MazF leads to the simultaneous selective synthesis of both "death proteins" and "survival proteins". *PLoS Genet.*, 5, e1000390.
33. Pellegrini, O., Nezzar, J., Marchfelder, A., Putzer, H. and Condon, C. (2003) Endonucleolytic processing of CCA-less tRNA precursors by RNase E in *Bacillus subtilis*. *EMBO J.*, 22, 4534-4543.
34. Schiffer, S., Rosch, S. and Marchfelder, A. (2002) Assigning a function to a conserved group of proteins: the tRNA 3'processing enzymes. *EMBO J.*, 21, 2769-2677.
35. Ochman, H. and Jones, I.B. (2000) Evolutionary dynamics of full genome content in *Escherichia coli*. *EMBO J.*, 19, 6637-6643.
36. Barker, M.M., Gaal, T., Josaitis, C.A. and Gourse, R.L. (2001) Mechanism of regulation of transcription initiation by ppGpp. I. Effects of ppGpp on transcription initiation in vivo and in vitro. *J. Mol. Biol.*, 305, 673-688.

37. Xiao, H., Kalman, M., Ikehara, K., Zemel, S., Glaser, G. and Cashel, M. (1991) Residual guanosine 3',5'-bispyrophosphate synthetic activity of *relA* null mutants can be eliminated by *spoT* null mutations. *J. Biol. Chem.*, 266, 5980-5990.
38. Laffler, T. and Gallant, J.A. (1974) Stringent control of protein synthesis in *E. coli*. *Cell*, 3, 47-49.
39. Hogg, T., Mechold, U., Malke, H., Cashel, M. and Hilgenfeld, R. (2004) Conformational antagonism between opposing active sites in a bifunctional RelA/SpoT homolog modulates (p)ppGpp metabolism during the stringent response [corrected]. *Cell*, 117, 57-68.
40. Ow, M.C. and Kushner, S.R. (2002) Initiation of tRNA maturation by RNase E is essential for cell viability in *Escherichia coli*. *Genes Dev.*, 16, 1102-1115.
41. Durfee, T., Hansen, A.M., Zhi, H., Blattner, F.R. and Jin, D.J. (2008) Transcription profiling of the stringent response in *Escherichia coli*. *J. Bacteriol.*, 190, 1084-1096.
42. Ross, W., Thompson, J.F., Newlands, J.T. and Gourse, R.L. (1990) *E.coli* Fis protein activates ribosomal RNA transcription *in vitro* and *in vivo*. *EMBO J*, 9, 3733-3742.

Table 3.1 Bacterial strains used in this study

Strain	Genotype	Source or reference
MC4100 Δ <i>mazEFG</i>	<i>araD139 D(argF-lac)205 flbB5301 ptsF25 rpsL150 deoC1 relA1</i> (8) <i>ΔmazEFG::kan</i>	
MG1693	<i>thyA715 rph-1</i>	<i>E. coli</i> Genetic Stock Center
W3110	<i>rph-1(rrnD-rrnE)1</i>	<i>E. coli</i> Genetic Stock Center
JW2753	<i>Δ(araD-araB)567 ΔlacZ4787(::rrnB-3) λ-<i>ΔchpA781::kan</i> <i>rph-1 Δ(rhaD-rhaB)568 hsdR514</i></i>	Keio collection (19)
SK4131	<i>ΔmazEFG</i> in MG1693 background	This study
SK4133	<i>ΔmazEFG rne-1</i> in MG1693 background	This study
SK4134	<i>pyrC::Tn10</i> in W3110 background	This study
SK4141	<i>ΔmazEFG rne-1</i> in W3110 background	This study
SK4142	<i>rne-1</i> in W3110 background	This study
SK4158	<i>rnz::apr</i> in W3110	This study
SK4159	<i>ΔmazEFG rnz::apr</i> in W3110 background	This study
SK4161	<i>ΔmazEFG rne-1 rnz::apr</i> in W3110 background	This study
SK4163	<i>rne-1 rnz::apr</i> in W3110 background	This study
SK4477	<i>Δrnz::apr rph-1</i> in MG1693 background	This laboratory
SK5664	<i>ΔpyrC::Tn10</i> in MG1693 background	This laboratory
SK5665	<i>rne-1</i> in MG1693 background	(18)
SK10165	<i>ΔmazF</i> in W3110	This study
SK10166	<i>ΔmazF rne-1</i> in W3110 background	This study
SK10167	<i>ΔmazF rnz::apr</i> in W3110 background	This study
SK10170	<i>ΔmazF rne-1 rnz::apr</i> in W3110 background	This study

Table 3.2. Oligos used in this study

Oligo name	Purpose	Sequence
mazEF 5'	Genotyping	5' ACCATCGACATGACCATTGA 3'
mazG	Genotyping	5' ATTAACCGTGGCAAACAGCA 3'
mazEF 3'	Genotyping	5' ATGGTGGCAAATGTCTGCTCATTA 3'
elaC-sense	Genotyping	5' CTAGAGCACTAGTATGAAACGTGATGAACTCATG 3'
elaC-antisense	Genotyping	5' ACTGCTCAAGCTTTTAAACGTTAAACACGGTG 3'
cspE-744	PCR for probe	5' TAAAGGTAACGTTAAGTGGT 3'
cspE-950	PCR for probe	5' GACGTATCTTACAGAGCGAT 3'
rpsO185A	PCR for probe	5' CTGAGTTTGGTCGTGACGC 3'
BrpsO-2	PCR for probe	5' GAGCTGCGTGTAACGTGCTA 3'

Table 3.3. mRNA half-lives of various strains containing the $\Delta mazEFG$ deletion in the W3110 genetic background.

Strain	Relevant genotype	Transcripts	
		<i>rpsO</i>	<i>cspE</i>
W3110	wild-type	1.4 ± 0.1^a	2.3 ± 0.5^a
SK4141	$\Delta mazEFG::kan rne-1$	3.3 ± 0.3^a	6.1 ± 0.4^a
SK4142	<i>rne-1</i>	5.4 ± 1.1^a	9.4 ± 0.1^a
SK4161	$\Delta mazEFG::kan rne-1 rnz::apr$	4.3 ± 0.6^a	4.7 ± 0.2^a
SK4158	$\Delta rnz::apr$	1.0^b	1.3^b
SK4163	<i>rne-1</i> $\Delta rnz::apr$	4.6 ± 0.2^a	12.1 ± 1.7^a
SK4159	$\Delta mazEFG::kan \Delta rnz::apr$	1.0^b	3.3^b

a. Half-lives represent the average of at least two independent determinations.

b. Half-life determinations were done just once.

Table 3.4. mRNA half-lives in $\Delta mazF$ strains

Strain	Relevant genotype	Transcripts	
		<i>rpsO</i>	<i>cspE</i>
W3110	wild-type	1.4 ± 0.1	2.3 ± 0.5
SK4142	$\Delta rne-1$	5.4 ± 1.1	9.4 ± 0.1
SK10166	$\Delta mazF::kan rne-1$	5.1 ± 0.8	9.5 ± 1.1
SK10170	$\Delta mazF::kan \Delta rnz::apr rne-1$	5.4 ± 0.1	13.5 ± 0.9

rpsO

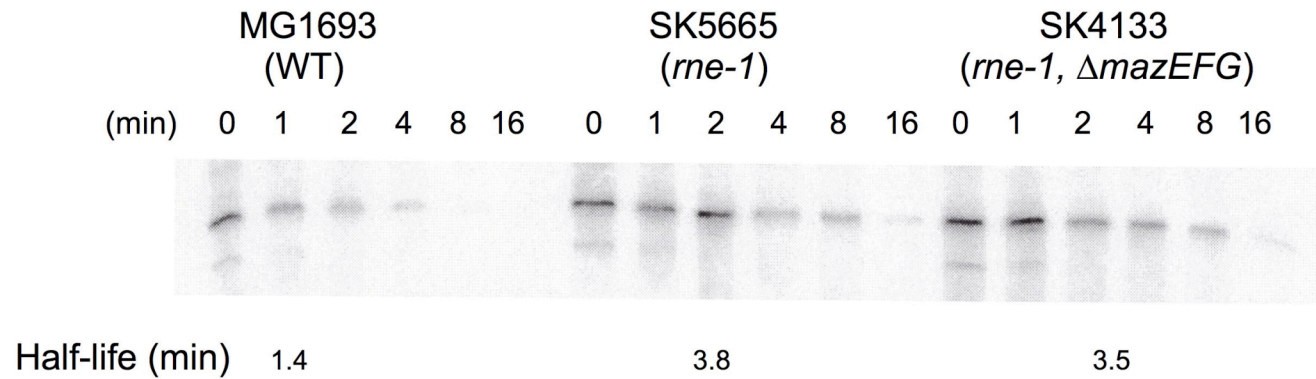


Figure 3.1. mRNA half-life of *rpsO* in $\Delta mazEFG$ deletion strains in the MG1693 genetic background. Experiment was performed only once.

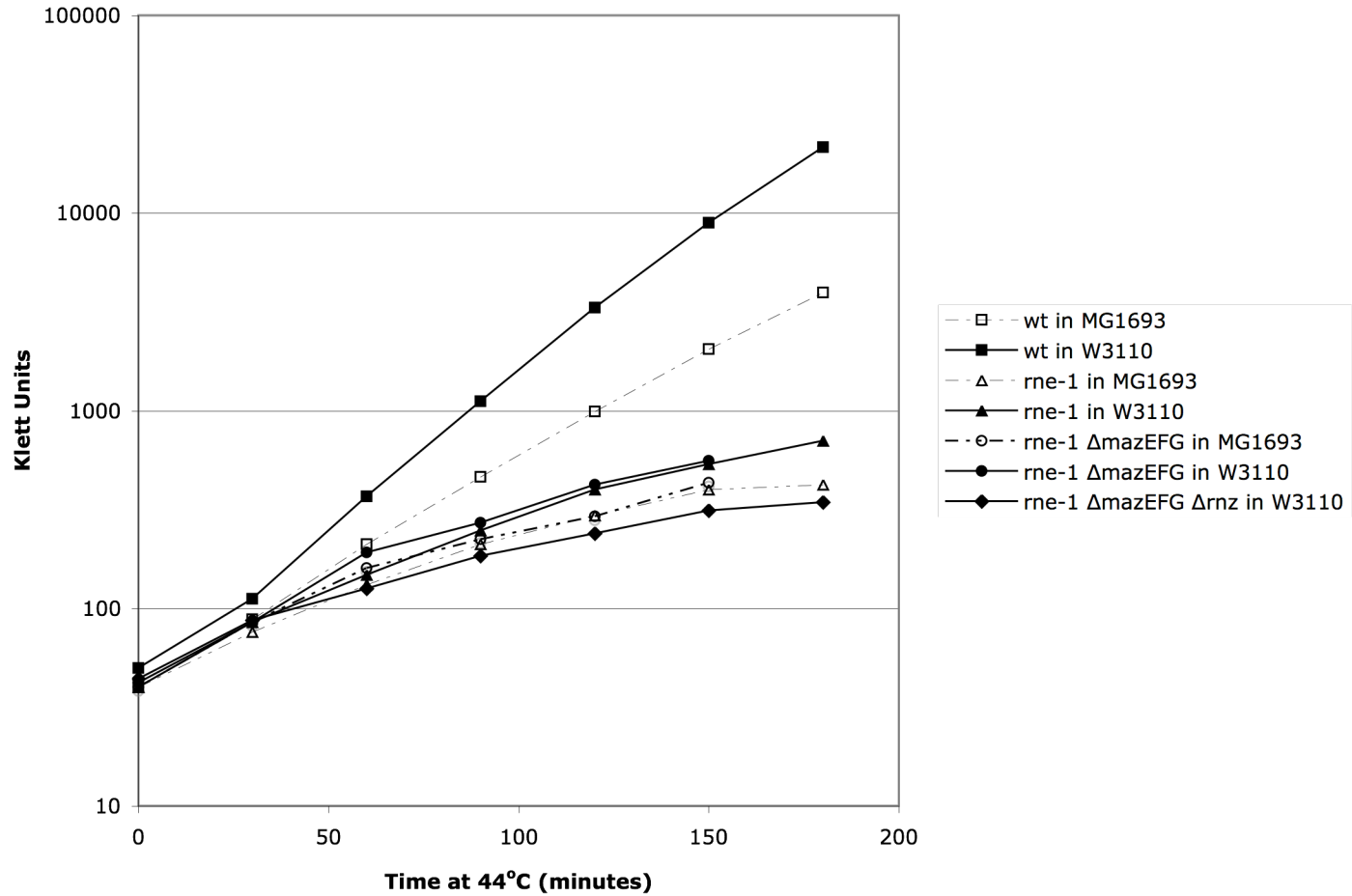


Figure 3.2. Comparison of growth properties of *rne-1* and *rne-1* $\Delta mazEFG$ mutant strains in the MG1693 (open symbols with dashed lines) and W3110 (solid symbols with continuous lines) backgrounds. Diamond shape is the *rne-1* $\Delta mazEFG$ Δrnz triple mutant in the W3110 background.

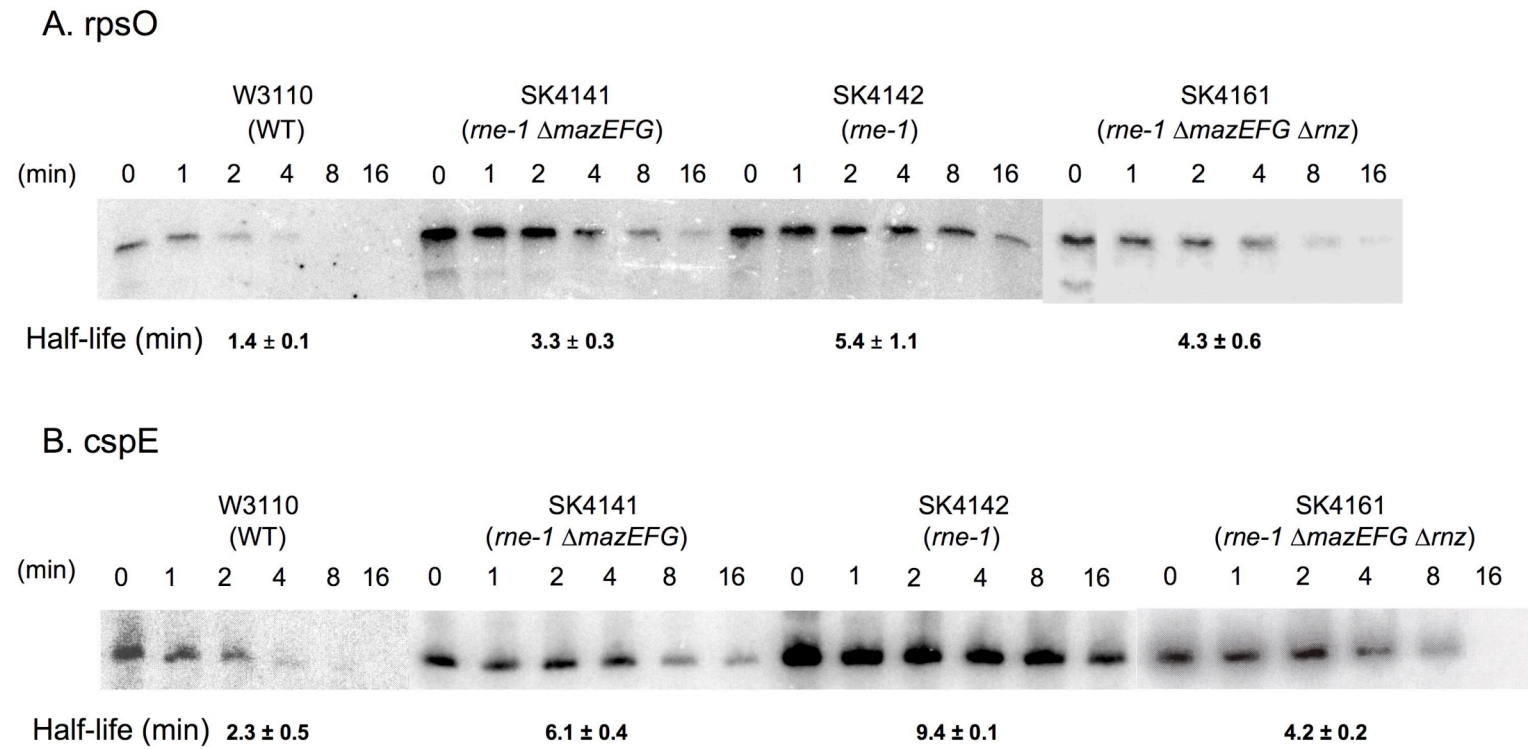


Figure 3.3. mRNA half-lives of *rpsO* and *cspE* in Δ *mazEFG* deletion strains in the W3110 genetic background. Data represents the average of at least two independent determinations.

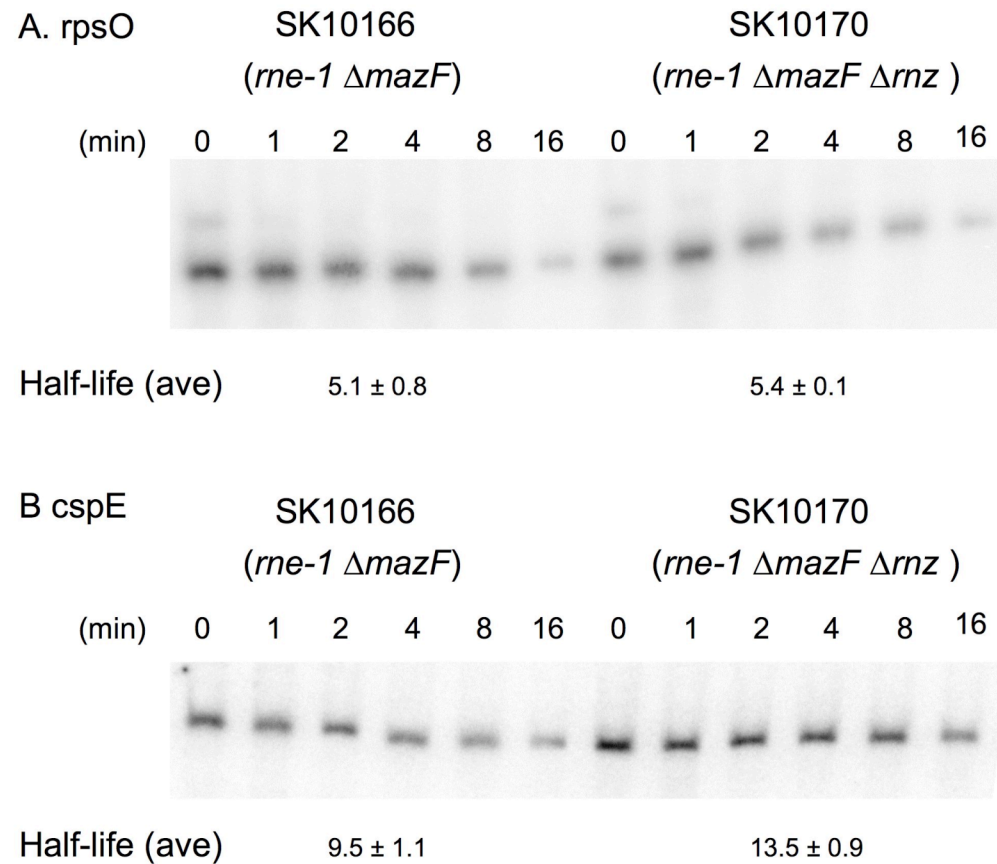


Figure 3.4. mRNA half-lives of *rpsO* and *cspE* in Δ *mazF* strains in the W3110 genetic background. Data represents the average of at least two independent determinations.

CHAPTER 4

CONCLUSIONS

The role of toxin-antitoxin (TA) systems as addiction modules that ensure plasmid maintenance via post-segregational killing (PSK) has been well established (1-3). These loci consist of a pair of genes encoding a stable toxic peptide and an unstable antitoxin. Due to their unstable nature, antitoxins need to be constantly expressed for continued inhibition of the deleterious effect of the toxins. In cells that fail to inherit the plasmid encoding the TA locus, the antitoxin pool is quickly degraded and, as a result, the toxin is free to act, killing the cells.

Toxin-antitoxin systems are also found in archeal and bacterial genomes (4). Since their discovery, the role of chromosomal TA systems has been the subject of great debate, but considerable evidence suggests that they are involved in several cellular functions including stress response, biofilm formation, persistence, and development (5-8).

Five classes of prokaryotic TA systems have been described thus far. They are characterized according to the nature and mechanism of action of the antitoxin. In type I TA systems, the toxin is inhibited by a small, regulatory RNA (sRNA) that binds to the mRNA of the toxic gene and prevents its translation (2). sRNAs can be divergently transcribed from the same locus as their target (*cis*-encoded) or they can be unlinked to their target genes (*trans*-encoded). The antitoxins of Type I TA systems found in plasmids are usually encoded in *cis* and, therefore, share extensive regions of

complementarity with their targets. The mechanisms by which several *cis*-encoded sRNAs regulate gene expression have been described. For the most part, binding of the sRNA to the target mRNA leads to RNase III-mediated cleavage of the RNAs.

In Chapter 2, we have characterized the role of several ribonucleases and the RNA chaperone Hfq in the biogenesis and decay of the sRNA SibC, a chromosomally encoded Type I antitoxin responsible for the regulation the expression of the toxin IbsC. This system is particularly interesting because the *cis*-encoded antitoxin sRNA has complete sequence complementarity to the mRNA of its target, the *ibsC* mRNA (9). We showed that the 3' end of SibC is processed by RNase E, RNase P, and RNase III to generate the three SibC transcripts that were observed in steady-state Northern blot analysis. We also demonstrated that these events were not the result of SibC/*ibsC* duplex processing as previously speculated (9). Furthermore, RNase III, RNase E, RNase P, as well as, Hfq impact the rate of SibC decay. Our data suggest that Hfq and RNase III protect SibC from degradation by RNase E. Hfq requires the C-terminal scaffold region of RNase E in order to protect SibC from RNase E activity. However, RNase E can act on SibC even when the C-terminal has been deleted. In addition, Hfq and RNase III mediate the destabilization of the *ibsC* mRNA. To the best of our knowledge, this is the first time Hfq has been shown to be required for mRNA degradation mediated by RNase III.

Our results expand the repertoire of roles for Hfq to include the regulation of gene expression mediated by *cis*-encoded sRNAs and suggest that the regulation of gene expression by *cis*-encoded sRNAs may share more features with *trans*-encoded sRNAs than previously thought. Further studies will need to be conducted to dissect the

mechanism by which SibC binding leads to IbsC inhibition and to determine unequivocally if the shorter form(s) of SibC are functionally active. In addition, it would be interesting to identify the physiological conditions under which SibC expression is downregulated and IbsC is released from inhibition. Understanding how the system is regulated may provide clues as to the biological importance of this chromosomal toxin-antitoxin system and its homologues.

Chapter 3 of this dissertation focused on a chromosomally encoded Type II toxin-antitoxin system. Unlike Type I TA systems, the toxins in Type II TA modules are inhibited by proteins that bind to and neutralize the toxic peptides. Here we analyzed the role of MazF in general mRNA decay in *Escherichia coli*. The *mazEFG* operon encodes the toxin MazF, an endoribonuclease that inhibits translation by cleaving mRNAs at ACA trinucleotides (10,11), its antitoxin MazE, and the nucleotide pyrophosphohydrolase MazG (12). Conditions that inhibit the expression of the MazE antitoxin, such as amino acid starvation, antibiotics that inhibit transcription and/or translation (i.e. chloramphenicol and rifampicin), as well as DNA damaging agents (i.e. nalidixic acid and mitomycin C), have all been shown to lead to MazF activation (13,14).

We examined if the presence of the MazF mRNA interferase affected the measurement of mRNA half-lives, since transcription initiation is inhibited in these types of experiments by the addition of rifampicin. Surprisingly, deletion of MazF did not lead to any change in the half-lives of two transcripts (*rpsO* and *cspE*) that contain multiple MazF cleavage sites (ACA sequences). However, deleting MazG led to significant alterations in mRNA half-lives. MazG helps regulate the stringent response by decreasing the levels of ppGpp, an alarmone that redirects the cellular machinery to decrease rRNA

and tRNA synthesis and increase biosynthetic pathways and transcription of stress-related genes to allow the cells to survive stressful conditions (12). Since our experiments were done under conditions in which RNase E, a major endoribonuclease involved in many aspects of RNA processing, was inactivated, it is possible that the stringent response was induced and that deleting MazG had an indirect effect on message decay. In fact, the transcription profile after stringent response activation shared numerous similarities with the transcription profile upon RNase E inactivation.

Interestingly, the effect of MazG in mRNA half-lives was observed in the W3110 genetic background but not in the MG1693 background. It would be interesting to further explore the link between the stringent response, MazG, and mRNA decay as well as the reasons behind the observed background differences.

REFERENCES

1. Gerdes, K., Larsen, J.E. and Molin, S. (1985) Stable inheritance of plasmid R1 requires two different loci. *J. Bacteriol.*, 161, 292-298.
2. Gerdes, K., Rasmussen, P.B. and Molin, S. (1986) Unique type of plasmid maintenance function: postsegregational killing of plasmid-free cells. *Proc. Natl. Acad. Sci. U S A*, 83, 3116-3120.
3. Ogura T, H.S. (1983) Mini-F plasmid genes that couple host cell division to plasmid proliferation. *Proc. Natl. Acad. Sci. U S A.*, 80, 4784-4788.
4. Yamaguchi, Y., Park, J.H. and Inouye, M. (2011) Toxin-antitoxin systems in bacteria and archaea. *Annu. Rev. Gen.*, 45, 61-79.

5. Buts, L., Lah, J., Dao-Thi, M.H., Wyns, L. and Loris, R. (2005) Toxin-antitoxin modules as bacterial metabolic stress managers. *Trends Biochem. Sci.*, 30, 672-679.
6. Gerdes, K., Christensen, S.K. and Lobner-Olesen, A. (2005) Prokaryotic toxin-antitoxin stress response loci. *Nat. Rev.*, 3, 371-382.
7. Nariya, H. and Inouye, M. (2008) MazF, an mRNA interferase, mediates programmed cell death during multicellular *Myxococcus* development. *Cell*, 132, 55-66.
8. Moyed, H.S. and Bertrand, K.P. (1983) *hipA*, a newly recognized gene of *Escherichia coli* K-12 that affects frequency of persistence after inhibition of murein synthesis. *J. Bacteriol.*, 155, 768-775.
9. Fozo, E.M., Kawano, M., Fontaine, F., Kaya, Y., Mendieta, K.S., Jones, K.L., Ocampo, A., Rudd, K.E. and Storz, G. (2008) Repression of small toxic protein synthesis by the Sib and OhsC small RNAs. *Mol. Microbiol.*, 70, 1076-1093.
10. Zhang, Y., Zhang, J., Hoeflich, K.P., Ikura, M., Qing, G. and Inouye, M. (2003) MazF cleaves cellular mRNAs specifically at ACA to block protein synthesis in *Escherichia coli*. *Mol. Cell*, 12, 913-923.
11. Aizenman, E., Engelberg-Kulka, H. and Glaser, G. (1996) An *Escherichia coli* chromosomal "addiction module" regulated by guanosine 3',5'-bispyrophosphate: a model for programmed bacterial cell death. *Proc. Natl. Acad. Sci. U S A*, 93, 6059-6063.
12. Gross, M., Marianovsky, I. and Glaser, G. (2006) MazG -- a regulator of programmed cell death in *Escherichia coli*. *Mol. Microbiol.*, 59, 590-601.

13. Sat, B., Hazan, R., Fisher, T., Khaner, H., Glaser, G. and Engelberg-Kulka, H. (2001) Programmed cell death in *Escherichia coli*: some antibiotics can trigger mazEF lethality. *J. Bacteriol.*, 183, 2041-2045.
14. Hazan, R., Sat, B. and Engelberg-Kulka, H. (2004) *Escherichia coli* mazEF-mediated cell death is triggered by various stressful conditions. *J. Bacteriol.*, 186, 3663-3669.